Fabrication of integrated microfluidic devices for Point-of-Collection analysis of biological and environmental samples

by

Feng Li

School of Natural Sciences

Submitted in fulfilment of the requirements for the

Doctor of Philosophy

University of Tasmania (January 2018)

Declaration of Originality

This thesis contains no material which has been accepted for a degree or diploma by the University or any other institution, except by way of background information and duly acknowledged in the thesis, and to the best of my knowledge and belief no material previously published or written by another person except where due acknowledgement is made in the text of the thesis, nor does the thesis contain any material that infringes copyright.

Authority of Access

The publishers of the papers in this thesis (comprising Preface, Chapters 1, and Chapter 3-5) hold the copyright for that content, and access to the material should be sought from the respective journals. The remaining non-published content of the thesis may be made available for loan and limited copying and communication in accordance with the Copyright Act 1968.

Statement of Ethical Conduct

The research associated with this thesis abides by the international and Australian codes on human and animal experimentation, the guidelines by the Australian Government's Office of the Gene Technology Regulator and the rulings of the Safety, Ethics and Institutional Biosafety Committees of the University. Ethics Approval Ref is H0010801.

Signed Feng Li

11th January 2018

Acknowledgement

Sincere appreciation to my supervisors, Professor Michael C. Breadmore, Professor Rosanne M. Guijt, and Dr. Niall P. Macdonald for offering me the great opportunity to be their PhD student. They were always ready to give me constructive advices for solving any scientific problems in my research with immense knowledge, and offer me positive encouragement to pursue my dream when I got lost about my future direction with patience and motivation. I could not have imagined having a better supervisor team for my PhD study. I would also like to extend my gratitude to my previous supervisors for my master study in Chongqing University (China), Professor Zhining Xia and Professor Fengqing Yang who gave me enormous support when I decided to further my PhD study in Australia.

I would also like to acknowledge all past and present Chippers & CEers group members and also the ACROSS members. There are several names I should highlight, Dr. Aliaa Shallan who helped and taught me a lot at the beginning of my PhD study, Dr. Petr Smejkal, Dr. Min Zhang (Professor Min Zhang soon), Dr. Joan Marc Cabot Canyelles, Dr. Yiing Chiing Yap, Dr. Hongheng See, and Dr. Sui Ching Phung who offered me continuous help to solve technical problems during my research.

Many thanks to CSL members, Mr. Paul Waller from the electric workshop, Mr. Christopher Broinowski from the mechanical workshop, and Dr. Karsten Goemann for taking SEM images.

I would also like to thank my "bushwalking, fishing, gym" mates, Min, Yabin, Yan, John, Mingxin, Joan Marc, Eli, Petr, Liang, you all made my PhD life full of joy, not just the "boring" lab work.

Last but not least, my deepest gratitude goes to my family members, my mom and dad for raising me up and supporting me through my life. Special thanks to my wife Jingxi Fan for her sacrifice and her utmost loving support.

Statement of Co-Authorship

The following people and institutions contributed to the publication of work undertaken as part of this thesis:

Candidate	Feng Li, School of Natural Sciences-Chemistry, UTAS
Author 1	Michael C. Breadmore, School of Natural Sciences-Chemistry, UTAS
Author 2	Rosanne M. Guijt, Centre for Rural and Regional Futures, Deakin University
Author 3	Niall P. Macdonald, School of Natural Sciences-Chemistry, UTAS
Author 4	Petr Smejkal, School of Natural Sciences-Chemistry, UTAS

Author details and their roles:

Book Chapter, <*Lab on a chip for point-of-care analysis of drugs in body fluids*>:

Located in Preface and Chapter 1

Candidate was the primary author (75%) and with author 1 and author 2 assisted with refinement and presentation.

Paper 1, <*Nanoporous membranes for microfluidic concentration prior to electrophoretic separation of proteins in urine*>:

Located in Chapter 3

Candidate was the primary author (75%) and with author 1 and author 2 assisted with refinement and presentation.

Paper 2, <*One-step fabrication of a microfluidic device with an integrated membrane and embedded reagents by multimaterial 3D printing*>

Located in Chapter 4

Candidate was the primary author (70%) and with author 1, author 2, author 3 and author 4 assisted with refinement and presentation.

Paper 3, <*Using Printing Orientation for Tuning Fluidic Behavior in Microfluidic Chips Made by Fused Deposition Modeling 3D Printing*>

Located in Chapter 5

Candidate was the primary author (70%) and with author 1, author 2 and author 3 assisted with refinement and presentation.

Paper 4, <*3D Printing clinical diagnostic devices*>

Located in Chapter 6

Candidate was the primary author (75%) and with author 1, author 2 and author 3 assisted with refinement and presentation.

We the undersigned agree with the above stated "proportion of work undertaken" for each of the above published (or submitted) peer-reviewed manuscripts contributing to this thesis:

Signed:

Prof. Michael C. Breadmore	Prof. John Dickey
Supervisor	Head of School

School of Natural Sciences

University of Tasmania

Date: 23/1/2018

School of Natural Sciences

University of Tasmania

23/1/2018

List of Publications

Type of Publications	Number	References
Papers in refereed Journals & book chapters	5	[1-5]
Oral presentations at international conferences	5	[6-10]
Posters at national and international conferences	9	[11-19]

[1] **Li, F.**; Guijt, R. M.; Breadmore, M. C. Lab on a chip for point-of-care analysis of drugs in body fluids. In *Nanobiosensors for Personalized and Onsite Biomedical Diagnosis*; Chandra, P.; *Institution of Engineering and Technology (IET)*: London, **2016**, pp 421-442.

[2] **Li, F.**; Guijt, R. M.; Breadmore, M. C. Nanoporous membranes for microfluidic concentration prior to electrophoretic separation of proteins in urine, *Analytical Chemistry* **2016**, 88, 8257-8263.

[3] Breadmore, M.C., Wuethrich, A., **Li, F.**, Phung, S.C., Kalsoom, U., Cabot, J.M., Tehranirokh, M., Shallan, A.I., Abdul Keyon, A.S., See, H.H., Dawod, M., Recent advances in enhancing the sensitivity of electrophoresis and electrochromatography in capillaries and microchips (2014–2016), *Electrophoresis* **2017**, 38, 33-59.

[4] **Li, F.**; Smejkal, P.; Macdonald, N. P.; Guijt, R. M.; Breadmore, M. C. One-Step Fabrication of a Microfluidic Device with an Integrated Membrane and Embedded Reagents by Multimaterial 3D Printing, *Analytical Chemistry* **2017**, 89, 4701-4707.

[5] **Li, F.**; Macdonald, N. P.; Guijt, R. M.; Breadmore, M. C. Using printing orientation for tuning fluidic behaviour in microfluidic chips made by fused deposition modeling (FDM) 3D printing, *Analytical Chemistry* **2017**, 89, 12805-12811.

[6] **Li, F.**; Guijt, R. M.; Breadmore, M. C. Nanoporous membranes for microfluidic sample-in/answer-out assay of proteins in urine, *The 7th ANZNMF*, Brisbane, Australia. 21-23 March **2016**. (Oral)

[7] **Li, F.**; Smejkal, P.; Macdonald N. P.; Guijt, R. M.; Breadmore, M. C. Multimaterial 3D printing for functional microfluidic device fabrication, *The 2nd ACROSS International Symposium on Advances in Separation Science (ASASS 2)*, Hobart, Australia. 3-5 December **2016**. (Oral)

[8] **Li, F.**; Macdonald N. P.; Guijt, R. M.; Breadmore, M. C. Point-of-care analysis with integrated microfluidic devices, *The 46th International Symposium on High Performance Liquid Phase Separations and Related Techniques (HPLC)*, Jeju, South Korea. 5-9 November **2017**. (Oral)

[9] **Li, F.**; Macdonald N. P.; Guijt, R. M.; Breadmore, M. C. Printing orientation influences fluidic behavior in channels made by fused deposition modeling, *The 17th Asia-Pacific International Symposium on Microscale Separations and Analysis (APCE)*, Shanghai, China. 10-13 November **2017**. (Oral)

[10] **Li, F.**; Macdonald N. P.; Guijt, R. M.; Breadmore, M. C. Point-of-Care analysis of targets from complex biological and environmental samples by integrated micro/nanofluidic devices, *The 25th RACI Research and Development Topics Conference*, Hobart, Australia. 3-6 December **2017**. (Oral)

[11] **Li, F.**; Guijt, R. M.; Breadmore, M. C. Microfluidic devices with integrated nanochannels for sample-in/answer-out analysis of pharmaceuticals from body fluids, *The 6th Australia & New Zealand Nano-Microfluidics Symposium (ANZNMF)*, Melbourne, Australia. 31 March-02 April **2015**. (Poster)

[12] **Li, F.**; Smejkal, P.; Guijt, R. M.; Breadmore, M. C. One-Step fabrication of a microfluidic device with an integrated membrane by multimaterial 3D printing, *The 20th International*

Conference on Miniaturized Systems for Chemistry and Life Sciences (μTAS), Dublin, Ireland. 9-13 October **2016**. (Poster)

[13] Phung S. C.; **Li, F.**; Macka M.; Powell S. M.; Guijt, R. M.; Breadmore, M. C. Multimaterial 3D printing: Integrated electrodes for ITP of bacterial cells, *The 20th μTAS*, Dublin, Ireland. 9-13 October **2016**. (Poster)

[14] **Li, F.**; Smejkal, P.; Macdonald N. P.; Guijt, R. M.; Breadmore, M. C. One-step fabrication of a microfluidic device with an integrated membrane and embedded reagents by multimaterial 3D printing, *The 8th ANZNMF*, Hobart, Australia. 26-29 June **2017**. (Poster)

[15] Islam, M. F.; **Li, F.**; Guijt, R. M.; Breadmore, M. C. A sample-in/answer-out device for the analysis of pharmaceuticals in biological fluids, *The 8th ANZNMF*, Hobart, Australia. 26-29 June **2017**. (Poster)

[16] **Li, F.**; Macdonald N. P.; Guijt, R. M.; Breadmore, M. C. Fabrication of an integrated microfluidic device using multimaterial 3D printing for point-of-care detection of drugs in body fluidis, *The 21st μTAS*, Savannah, USA. 22-26 October **2017**. (Poster)

[17] **Li, F.**; Macdonald N. P.; Guijt, R. M.; Breadmore, M. C. Printing orientation influences fluidic behavior in channels made by fused deposition modeling, *The 21st μTAS*, Savannah, USA. 22-26 October **2017**. (Poster)

[18] **Li, F.**; Macdonald N. P.; Guijt, R. M.; Breadmore, M. C. Tunable fluid mixing in 3D printed microfluidic chips fabricated with various printing orientations, *The 46th HPLC*, Jeju, South Korea. 5-9 November **2017**. (Poster)

[19] **Li, F.**; Macdonald N. P.; Guijt, R. M.; Breadmore, M. C. Fabrication of an integrated microfluidic device using multimaterial 3D printing for point-of-care detection of drugs in body fluidis, *The 17th APCE*, Shanghai, China. 10-13 November **2017**. (Poster)

List of Abbreviation

3D	Three dimensional
ABS	Acrylonitrile-butadiene-styrene
BET	Brunauer–Emmett–Teller
BGE	Background electrolyte
BSA	Bovine serum albumin
CAD	Computer-aided design
CCD	Charge coupled device
CE	Capillary electrophoresis
CFD	Computational fluid dynamics
DBS	Dried blood spots
DMF	Digital microfluidics
ECL	Electrochemiluminesence
EOF	Electroosmotic flow
EDL	Electric double layer
EDTA	Ethylenediaminetetraacetic acid
EME	Electro membrane extraction
FASI	Field amplified sample injection
FASS	Field amplified sample stacking
FDM	Fused deposition modelling
FITC	Fluorescein isothiocyanate
GC	Gas chromatography
HEPES	4-(2-hydroxyethyl)piperazine-1-ethanesulfonic acid
HPLC	High performance liquid chromatography

HPMC	Hydroxypropylmethyl cellulose
HSA	Human serum albumin
ICP	Ion concentration polarization
ITP	Isotachophoresis
LE	Leading electrolyte
LIF	Laser induced fluorescence
LLE	Liquid-liquid extraction
LOC	Lab-on-a-chip
LOD	Limit of detection
LOQ	Limit of quantitation
MEMS	Microelectromechanical systems
MMSL	Multimaterial stereolithography
MS	Mass spectrometry
NED	N-(1-Naphthyl) ethylenediamine dihydrochloride
PC	Polycarbonate
PCR	Polymerase chain reaction
PCTE	polycarbonate track etched
PDMS	Poly(dimethylsiloxane)
PLA	Poly(lactic acid)
PMMA	Poly(methyl methacrylate)
POC	Poin-of-collection
PolyJet	Photopolymer inkjet printing
PP	Polypropylene
PVP	Polyvinyl pyrrolidone

qPCR	Quantitative polymerase chain reaction
RSD	Relative standard deviation
R6G	Rhodamine 6G
SDS	Sodium dodecyl sulphate
SEM	Scanning electron microscope
SLA	Stereolithography
SLS	Selective laser sintering
SMT	Size/mobility trap
SPE	Solid-phase extraction
TDM	Therapeutic drug monitoring
TE	Terminating electrolyte
tITP	Transient isotachophoresis
Tris	tris(hydroxymethyl)-aminomethane
UV	Ultraviolet
µTAS	Micrototal analysis system
µPADs	Microfluidic paper-based analytical devices

Abstract

Lab-on-chip systems, also known as micro total analytical systems (μTASs), were introduced in late 80's, and are widely used in analytical chemistry for biological and environmental analysis. Sample preparation is often the most complex andcritical step in analysis – required to eliminate the large number of components that may interfere with the target and to enrich the trace amounts to detectable levels. While sample pretreatment is often conducted off-line, which is usually very time-consuming and labour-intensive, it also has a significant risk of analyte loss, degradation of the sample, or the introductionof contaminants. Benefiting from the portability, compactness, high levels of integrating and automation, integrated microfluidic systems are providing an alternative for point-of-collection (POC) biological and environmental analysis without sample pretreament, mitigating the risks caused by off-line sample pretreatment. This thesis focuses on different integrated microfluidic systems using various manufacturing methods for direct biological and environmental analysis.

Chapter 1 offers an overview of the POC analysis of biological and environmental samples. It starts with POCT analysis of drugs in body fluids with microfluidic systems, both therapeutic and illicit drugs detection in various matrixes including blood, urine, saliva *etc.* are discussed. This is followed by a brief overview of POCT analysis of environmental samples, focusing on the use of microfluidic paper-based analytical devices(μPADs), Polydimethylsiloxane (PDMS) and 3D printed chips are also mentioned, highlighting the many advantages of 3D printing for microfluidic fabrication such as: cost-effectiveness, less time-consuming and labour-intensive, and especially suitable for complex and integrated microfluidic manufacturing.

Chapter 2 is a comprehensive review of 3D printed integrated microfluidic devices for chemical applications. Different 3D printing technologies including fused deposition modeling (FDM), Polyjet, Stereolithography (SLA) and others are demonstrated for integrated device manufacturing. In particular how 3D printing can integrate various functionalities (detection, sensor, membrane, *etc.*) into microfluidic devices using multi mateiral printing or post-print with assembly.

In Chapter 3, an integrated microfluidic device was fabricated by sandwiching two nanoporous polycarbonate track etched (PCTE) membranes with differently sized nanopores between PDMS slabs containing embedded microchannels. This device is developed to seamlessly integrate sample preparation, and electrophoretic separation of proteins. The application was for the sample-in/answer-out quantification of albumin in human urine within 2.5 min. Results showed an improvement in sensitivity of 500 fold compared to a normal pinched injection using fluorescence detection. While effective, this approach was time-consuming and labour-intensive due to the lithography fabrication process for PDMS chips, raising the question of whether there are easier, and better approaches to fabricate these types of devices.

In Chapter 4, a microfluidic device containing an integrated porous membrane and embedded liquid reagent was made by multi material 3D printing (3DP) with a single step in 30 min. The body of the device was printed in transparent acrylonitrile butadiene styrene (ABS), and contained a 400 μm wide membrane printed from a commercially available composite filament. Liquid reagents were integrated by briefly pausing the printing before resuming sealing the device. The devices were evaluated by the determination of nitrate in soil slurry containing zinc particles for the reduction of nitrate to nitrite for colourimetric detection using the Griess reagent.

Fluid behaviour is significant in microfluidics, as laminar flow is preferable in some applications, while rapid fluid mixing is desired in others. Chapter 5 presents an simple way to tune the fluid mixing in microfluidic chips made by FDM 3D printing by varying the printing orientations. Devices were printed with filament orientations at 0°, 30°, 60°, and 90° to the direction of the flow. The FDM printed devices with 60° orientation showed the highest mixing efficiency, while 0° and 90° orientations printed chips had the least mixing, thus more laminar fluidic behaviour. Interestingly a rotational fluid flow was also obtained with the 30° chip. Two chips with laminar flow (0° filament direction) or mixing flow (+37/−37° filament direction) were used to perform isotachophoresis and colorimetric detection of iron in river water respectively, demonstrating the simplicity with which the same device can be tuned for different applications simply by controlling the way the device is printed.

Based on the results of previous chapters, in Chapter 6 an integrated microfluidic device was fabricated with materials of different functionality. Two membranes with different pore sizes (for extraction, purification, and concentration), and electrodes (for electrokinetic transport) were integrated within a transparent microfluidic body using a 5-head multi material FDM printer in a single fabrication process. The utility of the device was shown by directly measuring the ampicillin level in urine within 3 minutes, and a linear range of 0-100 ppm, showing the potential for low-cost POC diagnostics.

In Chapter 7, the findings of this research project are summarized and future directions suggested. This project developed an integrated microfluidic device, and achieved sample-in/answer-out analysis without sample pretreatment, demonstrated by analyzing both biological and environmental samples.

Table of content

The preface and chapter 1 have been removed for copyright or proprietary reasons.

They have been published as: Li, F., Guijt, R. M., Breadmore, M. C., Lab on a chip for point-of-care analysis of drugs in body fluids, in, Nanobiosensors for personalized and onsite biomedical diagnosis, The Institution of Engineering and Technology, P Chandra (ed), United Kingdom, pp. 421-442. ISBN 978-1-84919-950-6 (2016)

Chapter 2
Integrated 3D printed devices for chemical applications

1. Introduction

Integrated devices incorporate many functional components, performing multiple tasks in a single device instead of various separated ones. One of the best examples of an integrated device is an integrated circuit (IC), which was first reported by Kilby in the 1960s.[1] An IC is a small chip made with semiconductor material, normally silicon, with an integrated set of electronic circuits on it. Compared with the construction of discrete electronic components, ICs show huge advantages in cost and performance, attributing its dominating role in computers, mobile phones, and other electronic devices. Inspired by the IC industry, Microelectromechanical systems (MEMS) were also developed and widely utilized in microsensors, microactuators, and microsystems. Similar manufacturing techniques such as photolithography, etching, and deposition are used to fabricate MEMS.[2] They normally have moving components, thus allowing physical or analytical functions to be performed by the device in addition to their electrical functions.[3] MEMS facilitated the development of the integrated microfluidic device (also called lab-on-chip or miniaturized total analysis systems) by Manz and co-workers in the early 1990s.[4] Integrated microfluidic devices have been used in biochemical detection,[5-7] genetic analyses,[8-10], environmental analysis[11-13], as well as for cell culture and organic synthesis.[14,15]

The fabrication methods for microfluidic devices were initially inspired by the MEMS industry, including photoilithography, etching and deposition, and quickly expanded from glass and silicon to polymer processing approaches including casting, hot embossing and injection molding.[16] Three-dimensional (3D) printing or additive

manufacturing is a layer-by-layer process. Compared to conventional manufacturing methods, its merits include the more efficient fabrication of complex and bespoke designs, including those with integrated functionality. It has gained popularity in academic laboratories and has found applications in bioengineering,[17,18] microfluidics,[19-23] biochemical analysis,[24,25] and environmental analysis.[26,27]

2. The significance of utilizing 3D printing for fabricating integrated devices

3D printing was developed in the early 1980s, and used to make prototypes rapidly, and inexpensively at the early stages of development. With the improvement of the spatial resolution, and development of various printing materials including, plastics, resins, and metals, it has received considerable attention as manufacturing alternative. 3D printing has found applications in electronic engineering,[28-31] biomedical engineering,[32-34] aeronautical engineering,[35,36] tissue engineering,[37,38] biological,[39,40] medicine,[41,42] chemistry,[7,16,43-45]

The most widely used 3D printing techniques include stereolithography (SLA), fused deposition modeling (FDM), inkjet printing, laminated object manufacturing (LOM), selective laser sintering (SLS), and direct writing.[46,47] Each 3D printing technique has its own merits and drawbacks in terms of fabrication speed, resolution, accuracy, and cost; comprehensive comparisons have been made by some excellent reviews.[16,19,23,48] For integrated device fabrication, FDM, Polyjet, and SLA are used most , and three approaches of integration can be distinguished: (1) Single material 3D printing (2) Print-pause-print (PPP) 3D printing, and (3) Multimaterial 3D printing. Focusing on integrated devices, 3D printing offers advantages including rapid validation of design, cost-effective equipment,

freeform fabrication of 3D geometries, and of particular importance from the microfluidic perspective it closes the gap between materials used in academia (PDMS) and commercial manufacture (thermoplastics including PMMA, COC and polystyrene).[49]

3. Recent developments of 3D printed integrated devices in chemical applications

3D printing has been used by the research community for the fabrication of integrated devices for various chemistry applications, such as chemical synthesis,[50,51] electrochemical detection,[52,53] and sensing.[54,55] In this section, we review papers published in recent years that used 3D printing to fabricate a diverse range of integrated devices for chemical applications. Reviewed works are categorized based on the integration methods (Single material 3D printing, PPP 3D printing, and multimaterial 3D printing) and the integrated functionalities including: pumps, valves and mixers, electronics, modular microfluidics, membrane and porous structures, and chemical reactants. Table 1 summarizes all integrated devices discussed in this review, highlighting the integrated functionalities, applications, materials, and the 3D printing technologies that was used.

3.1 Functionally integrated devices by single material printing

Currently, most 3D printing methods manipulate only one single material due to the technical difficulty in realising multimaterial printing for some printing approaches and the limited range of materials available for most of the printer types. Single material 3D printing can fabricate functionally integrated devices by utilizing intrinsic properties of printing materials, such as elasticity,[56,57] or porosity,[58-60] or by adding functionality

through geometric design,[21,61,62] as well as by constructing reconfigurable modular devices from discrete elements.[63,64]

3.1.1 Valves, pumps, and mixers

Valves, mixers, pumps and are usually an essential part for fluid manipulation in analytical systems. Rogers and co-workers fabricated a microfluidic device with integrated valves that demonstrated for up to 800 actuations, which was the first reported 3D printed valves. The microfluidic device including the membrane was 3D printed with a customize resin mainly contains Poly(ethylene glycol) diacrylate (PEGDA) using a SLA printer. The membrane was approximately 100 μm, and suspended over a valve chamber. The membrane was deflected when an external pressure was applied to the valve chamber until it seals the inlet and outlet openings to close the valve, while the membrane returned to its original position when the pressure was released to open the valve.[43] To enhance the performance of the valves, Gong *et al*. from the same group modified the SLA resin by adding a thermal initiator, and successfully fabricated a robust and miniaturized 3D printed microfluidic device with integrated valves and pumps. As the valve volume was only 10% of that in their previous report, and the durability was improved from 800 actuations to 1 million actuations. Pumps and mixers were also constructed by combining valves with displacement chambers.[57] Similarly, Au and co-workers 3D printed microfluidic devices with integrated valves and pumps by incorporating 3D printed membrane in the microfluidic devices as shown in Figure 2.1. The performance of the membrane to different pressure loadings was firstly simulated using COMSOL software to calculate maximum pressure before deformation, and confirmed with experimental studies.[44]

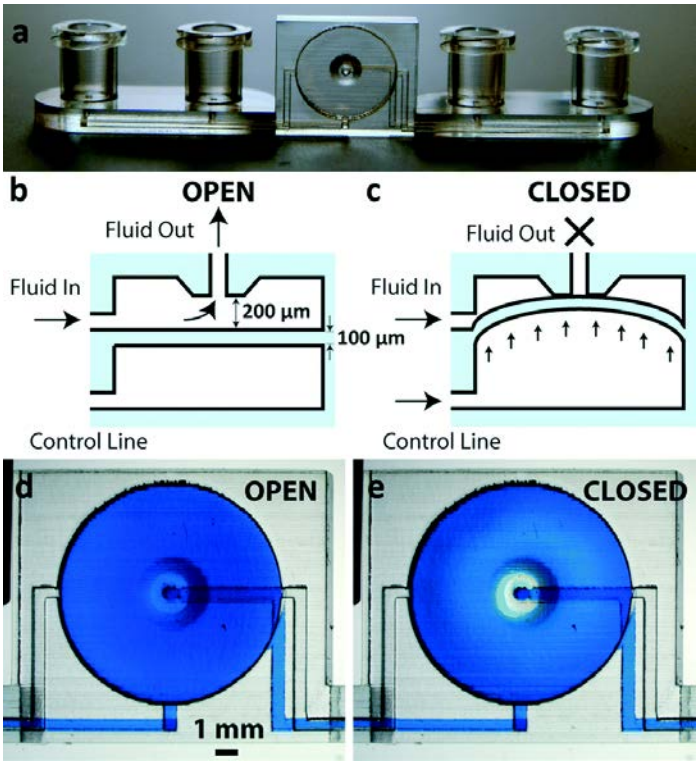

Figure 2.1 Basic valve design. (a) Photograph of the single-valve device. (b, c) Schematics of a valve unit in its open (b) and closed (c) states. (d, e) Micrographs of a valve unit in its open (d) and closed (e) states. Reproduced from [44] with permission from the Royal Society of Chemistry.

Traditional instruments housed in centralized laboratories typically control the fluid by utilizing pressure, which is reliable and has a rapid response time, but requires bulky external equipment such as syringe pumps or gas pressure line. Wang *et al.* developed a 3D printed peristaltic microfluidic system comprising micropumps and micromixer for detection of low-level insulin concentration using a chemiluminescence immunoassay. The micropumps and micromixer were fabricated using a FDM printer printing with a flexible material thermoplastic elastomer (TPE), which can be pneumatically controlled for pumping and mixing sample fluids. The 3D printed micropumps and micromixer showed comparable fluid control results with PDMS devices.[56] The 3D printing resolution allowed for the fabrication of a thin membrane, which can be actuated and controlled by pressure, functioning as a valve or pump. 3D printed microfluidic devices with integrated valves and pumps were used for culturing and observation of CHO-K1 cells; facilitated by the optically transparency and biocompatibility of the 3D printing resin (Watershed XC 11122, DSM Somos).[44]

Valves and pumps actuated by rotating or torqueing were also 3D printed using a SLA printer by Chan *et al*. The pumps and valves mainly consisted of two parts including a screw and main chip piece, controlled by rotating the screw to different directions and extent. By integrating with microfluidic components, these devices were used to perform colorimetric assay of proteins in urine using a smartphone as the imaging platform. Data processing was carried out on a laptop after transfering the images. The whole assay was done within 25 minutes, and chip cost of US$0.22 without any extra lab instruments (pumps, gas pressure sources, microscopes). Recognising that in comparison with a lateral flow assay, the device is more complex and more expensive, the quality of the data obtained using limited infrastucture highlight the potential of 3DP microfluidics, for advanced point-of-care analysis in resource-limited areas. [65]

Microfluidic mixing is required for many processes, including chemical reactions,[66,67] and biochemical assays.[68,69] Mixing can be achieved by passive (diffusion, chaotic) or active (pumps, surface acoustic waves, internal moving components) methods.[70] The ability of creating complex geometries in a single manufacturing step makes 3D printing an efficient way to fabricate mixers in comparison to traditional microfabrication methods. An auto-mixing chip based on capillary forces was 3D printed by Plevniak and co-workers using a PolyJet printer. The device comprised a ring-shaped mixing channel by combining a 'Slit and Recombination (SAR)' structure with serpentine channels. Fast (~1 s) and complete fluid mixing was observed, with CFD simulations experimentally confirmed. By integrating this chip with a smartphone, the device was used for point-of-care diagnosis of anaemia by colorimetric quantification of blood hemoglobin levels.[71] A Baker's transformation was proposed as a 3D micromixer of sequential symmetrical units by Carrière.[72] Based on this transformation, Shallan *et al.* fabricated a micromixer showing complete fluid mixing of two different dyes, fluorescein and rhodamine B utilizing a DLP-SLA printer.[21] To further explore the application of this 3D printed micromixer based on Baker's transformation, Cabot *et al.* integrated the 3D printed mixer with capillary electrophoresis for high-throughput determination of acidity constants (pK_a) within 2 min. Four different reagents were pumped to the micromixer for complete mixing into one single homogenous flow. Buffers with various pH (2-13) and ionic strength were obtained in aqueous media and several methanol–water mixtures. This device can be used as a rapid, simple, and flexible method for determining pK_a values of pharmaceutical targets.[73] A 3D printed preconcentrator with ordered cuboids in the extraction channel to improve liquid mixing was developed by Su and co-workers. The whole device containing 526 cuboids in the channel was 3D printed using a SLA printer, and then was integrated with a flow injection system for selective preconcentration of trace metal ions

in seawater. The authors believed that the extraction of metal ions by the 3D printed device was achieved by polymer-metal ion interaction. Finally the system was combined with ICP-MS for metal ions quantification.[26] Microfluidic mixers with different structures were also fabricated in glass using femtosecond laser direct writing. As the optical transmission of glass is greater than that of 3DP materials, these micromixers would be an idea candidate when optical detection is required.[74]

In addition to using complex geometries, fluid mixers can be constructed by changing the layout of material when 3D printing. Macdonald *et al.* compared three different 3D printing methods, SLA, FDM, PolyJet for the fabrication of microfluidic devices. Fluid mixing in microchannels fabricated with these three 3D printing methods was compared using a simple "Y" shape chip, and it was found that FDM provided highest fluid mixing, and then followed by PolyJet and SLA. Fluid mixing was related with the surface roughness, and FDM chip produced roughest surface and was considered to be the best option for micromixer fabrication.[75] Li *et al.* further explored the impact of FDM printing orientation of the filament to control the fluid mixing as shown in Figure 2.2. Different printing orientations (0°, 30°, 60°, 90°) of the filament lay to the direction of the fluid flow were compared using the same "Y' chip design. Chips fabricated with 60° printing orientation were determined to be optimal for fluid mixing, and were used to detect iron in water by colorimetric assay. For chips fabricated at 0° to the lay, minimal mixing was observed compared to other printing orientations, and was used for isotachophoresis.[62]

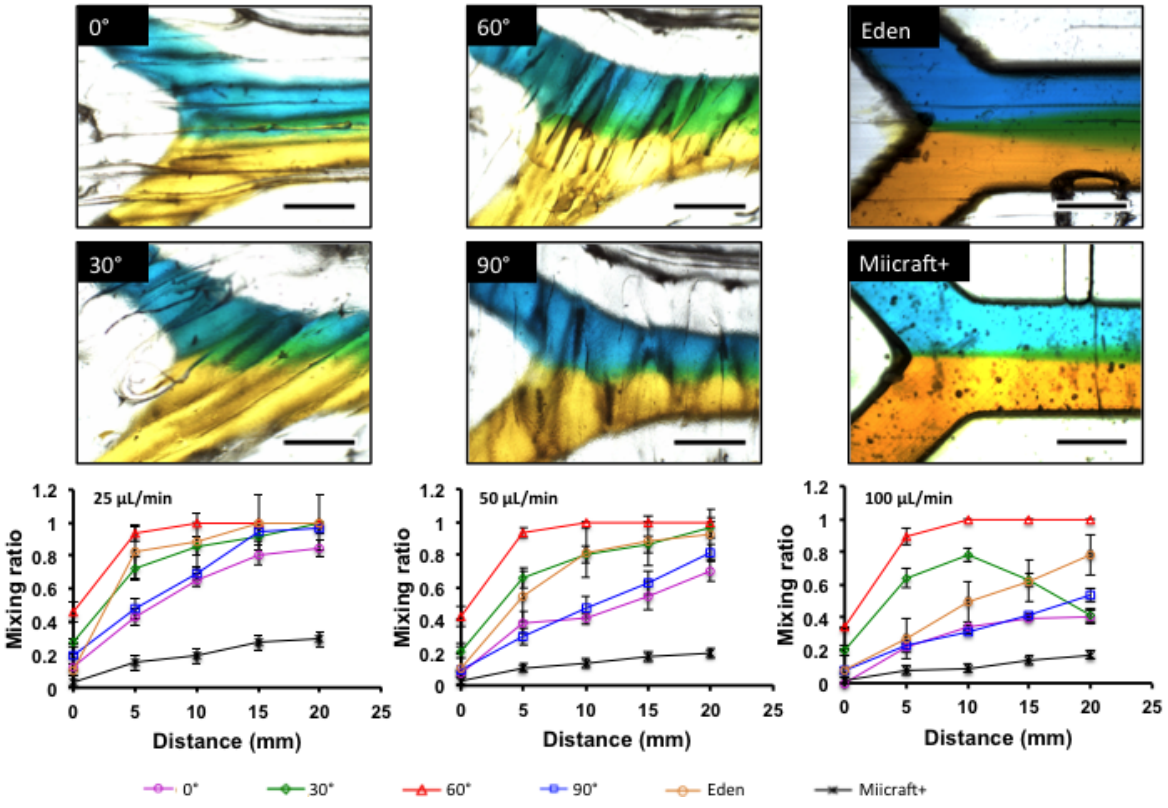

Figure 2.2 Microscopic images of laminar flow within 500 µm × 500 µm channels into 750 µm × 500 µm channels, visualized with yellow and blue food dye at 25 µL/min for FDM 0°,30°,60°, and 90°, Eden, and Miicraft+, respectively. Plots of distance vs mixing ratio, demonstrating diffusion through the laminar flow channel at 25, 50, and 100 µL/min are also shown below the microscopic images. N = 3, scale bar = 500 µm. Reproduced from [62] with permission from the American Chemical Society.

Similarly, fluid mixing in a microfluidic chip can also be controlled by simply orientating the chip at a certain angle relative to the gravity. Norouzi *et al.* accomplished the fluid mixing control in a SLA printed chip by holding the chip at various angles. A density difference of 2% of two fluids was required for fluid reorientation to occur. The mixer was capable of generating any desired mixing ration of two fluids without any external forces.[61]

3.1.2 Porous structures and membranes

Porous structures can be integrated by utilizing poriosity as material property or through fine-tuning 3D printing process. Planar chromatography is a widely used analytical technique in which the porous stationary phase is on a flat plate and the mobile phase moves through stationary phase though capillary action. Fichou and co-workers developed a 3D printed planar chromatography in silica gel. A modified FDM printer was used to directly print the chromatography plate with silica gel, the separation performance of this chromatography method was confirmed by the separation different dyes with results comparable to a commercial TLC plate. Benefiting from the freedom of the 3D design, this method offered new potential in terms of geometry, shape and functional integration; potentially extending from 2D to 3D chromatography.[60] Similarly, Macdonald *et al.* fabricated a microstructured surface for TLC using a PolyJet 3D printer as shown in Figure 2.3. The specific microstructure was printed by tayloring printing process and orientation, with devices printed parallel to the print head showing better results characterized by shorter separation time and reduced interference form the adjacent channels. The surface was found to be negative charged when it was used for two water-soluble dyes, phenol red and bromothymol blue. Finally this device was used for separation of two proteins with different *pI* values, myoglobin (pI 6.8, 7.2) and lysozyme (pI 11.35), the lysozyme was retained on the original position due to the

positive charge, while the myoglobin moved through the plate by the capillary action.[58] Belka and co-workers 3D printed a porous sorbent for drug extraction using FDM printer. The material used in their research was LAY-FORMM 60, a material which becomes porous after removal of a water-soluble support by washing with water. They integrated the sorbent with an Eppendorf tube for centrifuge extraction of glimepiride from water, and the extraction efficiency reached 82.24% after 60 min.[59]

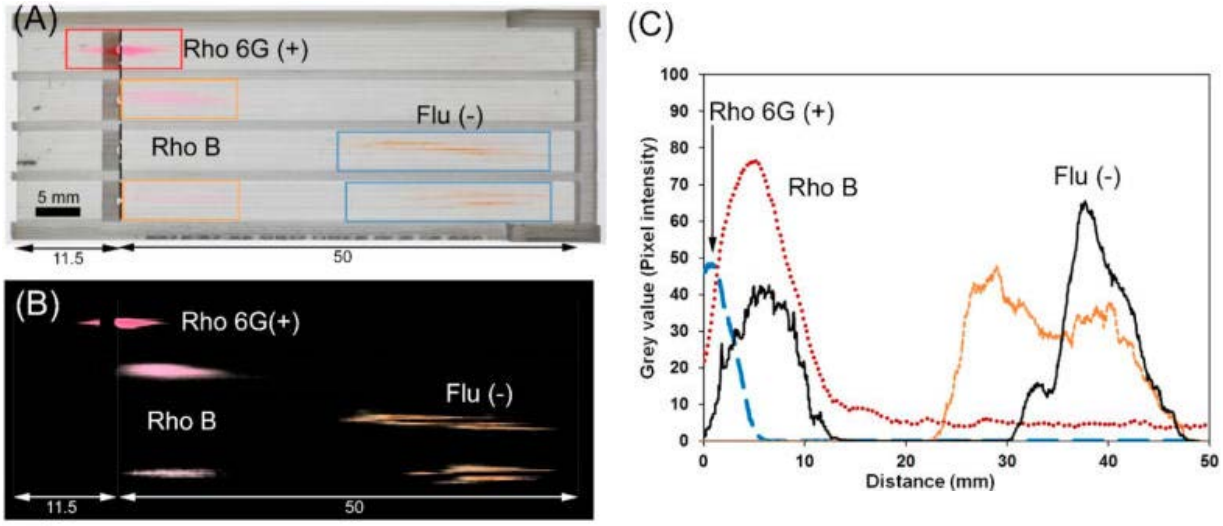

Figure 2.3 3D printed TLC chip showing separation of fluorescent dyes, namely rhodamine 6G (Rho 6G), rhodamine B (Rho B), and fluorescein (Flu). (A) Photograph showing the chip with separated dyes indicating their respective charges at basic pH. (B) Processed photograph with the background removed showing the separated dyes only. (C) Generated chromatogram from the processed image shown in part B. Reproduced from [58] with permission from the American Chemical Society.

3.1.3 Fluidic interconnects and modular systems

Typically, microfluidic systems are constructed in a monolithic form using various fabrication methods, including 3D printing. The design is typically tailored towards a specific microfluidic application and may contain multiple functional elements. This monolithic approach means that even for a slight modification in one of the functional elements, the entire microfluidic system needs to be re-made, increasing development time and cost. Modular microfluidics however involves the design and fabrication of individual microfluidic modules (channels, mixers, valves) before combining the functional elements into a system.[63,76-78] Bhargava and co-workers constructed several microfluidic based devices including gradient generator, microdroplet generator and optical droplet sensing system by integrating a sample library of SLA printed standardized components such as mixers, splitters, junctions *etc.* Various functional elements were printed using a SLA printer as shown in Figure 2.4. Assembly of the system from the functional units was realized using an approach similar to building with Lego®, and allowed for customized microfluidic design by assembly.[63]

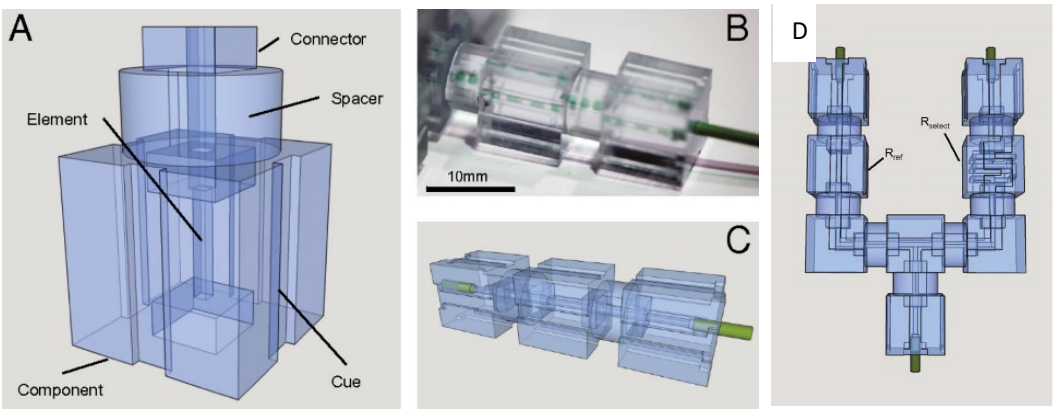

Figure 2.4 (A) CAD assembly drawing of a 1-mm male–male connector aligned with female-type port terminating a 750-μm microfluidic element of straight pass type. (B) The flat mating surfaces of the connector pin and port allow for easy optical inspection of the connector–element channel junction. (C) Chip-to-world interfacing is performed through a single component that reversibly seals to standardized 1/16" PEEK tubing. (D) CAD assembly drawing for a 2-input, 1-output concentration gradient generator in which a single branch resistor varies the mixing ratio. Reproduced from [63] with permission from the National Academy of Sciences.

Inspired by electronic circuit prototyping using breadboards and Lego®, Yuen presented a "plug-n-plug" modular microfluidic system. The "SmartBuild System" comprised of multiple microfluidic components were fabricated *via* a SLA printer. Various microfluidic elements including a motherboard with fluidic interconnects, fittings, and fluidic inserts were 3D printed before their assembly into a system.[77] Yuen presented a "stick-n-play" modular microfluidic system, which can be disassembled and assembled again for building different integrated microfluidic systems. The "stick" was a magnetic interconnect consisting of ring magnets and sealing gaskets fitted and glued into each module. The magnetic interconnect could reversibly "stick" microfluidic modules together to form an integrated microfluidic device.[78] Furthermore, a multidimensional modular microfluidic device was constructed by Yuen and co-workers.[79] Lee and co-workers fabricated modular microfluidic device for biosensing AFP biomarker, the microfluidic components were 3D printed before assembly using o-ring and metal pins.[76]

3.2 Functionally Integrated devices by PPP 3D printing

3D printing is typically a continuous process to build a model layer-by-layer. This process, however, can be paused mid-print to insert parts or hyphenate with a complementary fabrication processes to create hybrid devices. Hybrid 3D printing can also include traditional, subtractive manufacturing methods such as machining, cutting, dispensing, and robotic placement.[80] By taking advantage of the geometric benefits of 3D printing, and integrating other components into the fabrication process, additional functionality included in the final device. To date, various functional parts have been integrated through this PPP technique for microfluidic devices, including electronics,[81-83] chemical reactant,[84-86] and membranes.[87,88]

3.2.1 Sensors and electronics

Duarte and co-workers 3D printed a microfluidic device with embedded electrodes for generating, and measuring the size of microdroplets based on capacitively coupled contactless conductivity detection (C4D). The electrode was firstly printed with carbon nanotube-doped PLA in the bottom layer of the device, and then the filament was replaced by ABS to proceed with fabrication of microchannels through the same printing nozzle.[81] A 3D printed electronic tongue that can be used to distinguish tastes below the human threshold was built using a FDM printer through the PPP technique. In this case a gold inter-digitated electrode was embedded for taste sensing. The samples were 1 mM NaCl, HCl, caffeine and sucrose solutions. Electrical response of the analytes were acquired using a impedance analyzer, then the response of the sensor was analyzed using principal component analysis. Different solutions were differentiated using this electronic tongue showing a 99.98% correlation of tastants.[82] A water quality monitoring system integrated with miniaturized pH and conductivity sensors was fabricated *via* FDM printing, using PPP to embed the sensors. The pH sensor was based on a hydrogel, which could swell/de-swell according to the pH, leading to a change in the electrical properties (conductivity and capacitance) of the hydrogel. A conductivity sensor was made by embedding two interdigitated electrodes in a 3D printed interface . The performance of the sensor system was tested at different temperatures and flow rates, and experimental results agreed with the values predicted based on theory.[83]

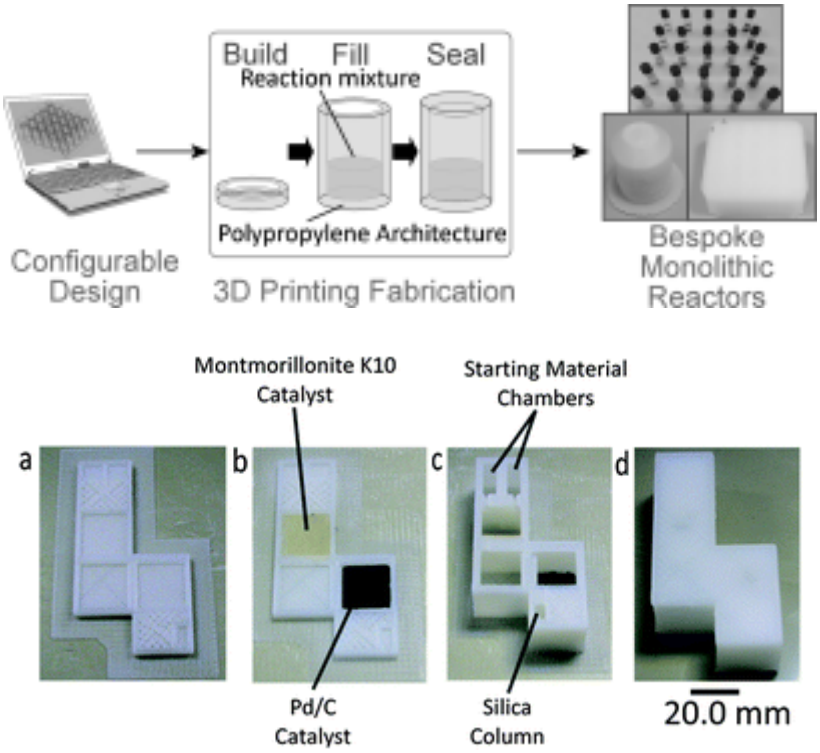

Figure 2.5 (Top) The laboratory manufacturing process of 3D printed sealed reactors for hydrothermal synthesis. (Bottom) (a) Reactor base with purification column before printing of catalyst regions. (b) Reactor base with purification column after printing of catalyst regions. (c) Fabricated reactor with purification column after addition of starting materials, reagents and packing of silica. (d) Final sealed reactor. Reproduced from [84-86] with permission from the Royal Society of Chemistry.

3.2.2 Chemical reactants

Multi-step chemical synthesis normally consists extensive protocols including, adding reactants and catalysts, purification and separation of products. This involves multiple manual handling steps, which in addition to exposure risks could potentially incur product loss, is prone to error and may increase time and cost. FDM printing was used to produce various kinds of reactionware for chemical synthesi. The PPP technique was used for the introduction of reaction mixtures and catalysts into the reactors. The geometry allowed for initiation and control of reactions using orientation as shown in Figure 2.5. By using this method, multi-step chemical synthesis was conducted with minimal chemical handling by the operator, allowing complex manipulations to be more precisely controlled, optimized, and shared with other researchers. This approach has also allowed the fabrication of customized chemical reactors which can be tuned by the individual researcher.[84-86] Scotti *et al.* FDM printed a polypropylene reactor using the PPP approach with an integrated stainless steel nanoelectrospray ionisation capillary and a magnetic stir bar for direct injection into a mass spectrometer for reaction monitoring. The device was used for monitoring a Diels–Alder reaction and the subsequent retro Diels–Alder reaction.[50] Lederle and co-workers 3D printed a NMR tube/spinner combinations with integrated reactants inside the inert-gas atmosphere of a glovebox for palladium-catalyzed decarboxylative Sonogashira coupling of aryl halides with arylpropiolic acids. Within the totally gas tight and pressure resistant tubes, a set of arylnaphthylalkynes was synthesized and the progress of the reaction was monitored *via* NMR spectroscopy.[89]

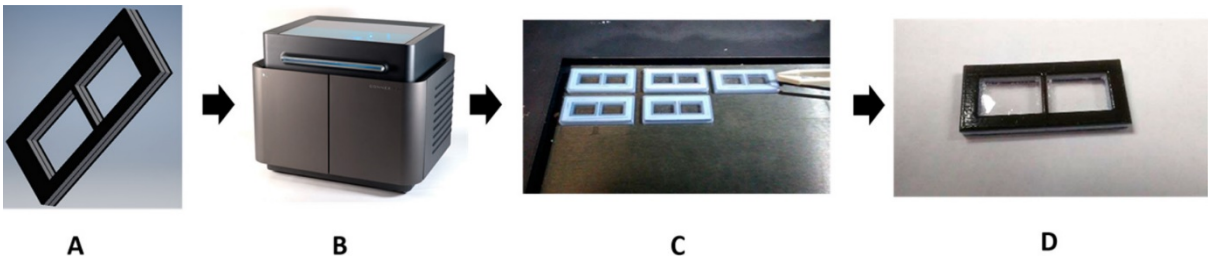

Figure 2.6 In panel (A), a model is drawn using Autodesk Inventor Professional 2017 CAD software. The model is saved as an .stl file and sent to the 3D printer (panel (B)). The membrane holder is printed with multiple materials. The interior is a rigid Verowhite material, and the exterior is a compressible TangoBlack material, to prevent leaking. In panel (C), the operator places the membranes into the device halfway through the print process. Panel D shows the final product: a membrane holder with a membrane seamlessly sealed into the device. Reproduced from [88] with permission from the American Chemical Society.

3.2.3 Porous structures and membranes

Yuen fabricated various fluidic devices with integrated porous membranes or light-diffusing fibers using PPP technique. A 3D printed fluidic device with an embedded porous membrane was used for continuous perfusion cell culture, and the integrated light-diffusing fiber offered opportunities in illumination or optical applications.[87] A commercial membrane was embedded in a printed equilibrium-dialysis device for investigating the binding of small molecules and ions to proteins. The PPP process is shown in Figure 2.6. The advantage of this method is that various pore sized membranes can be embedded for different applications. However alignment could be challenging, and there is difficultly in avoiding damage or contamination of the membrane when resuming printing.[88]

3.3 Functionally integrated devices by Multimaterial 3D printing

Multimaterial 3D printing, enabling the integration of functional parts with different material properties in a single run, is attractive for the manufacture of integrated devices. Chio and co-workers developed a multi-material stereolithography (MMSL) machine containing 4 resins. MMSL can produce unique multi-material complex parts that are functional and visually illustrative.[90] Multimaterial-inkjet based systems are much quicker, as the different materials can be printed in the same print pass for each layer.[91,92] For example, the Stratasys Objet Connex printers can print up to three different materials, and various combinations of these, in a single run. Multimaterial FDM printing has fewer obstacles to overcome than SL and inject printing, notably: (1) it does not require a support material, (2) the printed material is loaded as a solid, (4) has a wide range of materials, (5) which are typically thermoplastics.[19]

3.3.1 Valves, pumps, and mixers

Begolo *et al.* utilized a polyjet multimaterial 3D printer (Objet 260 system) to fabricate a pumping lid to achieve equipment-free pumping for microfluidic applications by controlled generation of pressure. Two materials with different mechanical properties (rigid and elastic) were simultaneously printed to make the pumping lid. One type of pumping lid they manufactured could produce predictable positive or negative pressure by controlling the compression and expansion of gases. A theoretical model was developed to describe the pressures and flow rates generated with this approach, and it was also validated experimentally. The other type relied on a vapor–liquid equilibrium to generate pressure, and it was validated by controlling flow into droplet microfluidics, laminar flow chips, and also loading sample in a commercial chips.[93] However, the pumping lid they developed was only used to compress air, and was not applied to pump water fluids directly. So Jue and co-workers from the same group used the same multimaterial 3D printing method to fabricate an interlock meter-mix device as shown in Figure 2.7. Different from the previous pumping lid, which was used to compress air without contacting the fluid directly, this meter-mix device can generate sealed fluid cavities for accurately metering of urine and completely mixing it with lysis buffer without an external device. This type of device has potential in point-of-care analysis in resource-limited areas.[94]

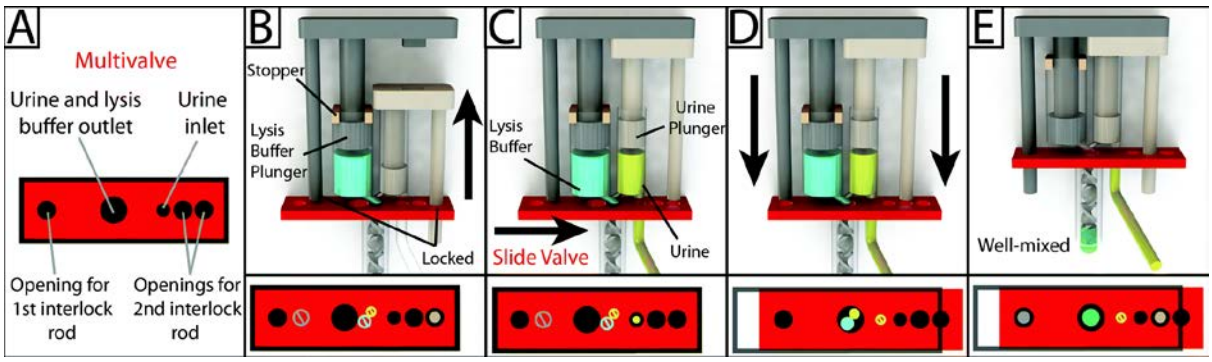

Figure 2.7 Schematic overview of the design and operation of the 3D-printed interlock meter-mix device for metering and mixing a urine sample with lysis buffer. (A) The multivalve has five holes that are labeled accordingly. (B) Lysis buffer (blue) is preloaded into the lysis buffer chamber, where the topmost position of the lysis buffer plunger (left, grey) is pre-determined by stoppers (tan). The urine plunger interlock rod (right, beige) is positioned within the multivalve, preventing the valve from sliding and simultaneously blocking the lysis buffer plunger interlock rod. The user pulls up on the urine plunger (C) until it contacts and is stopped by the lysis buffer plunger, aspirating urine and simultaneously removing the urine plunger interlock rod from the multivalve. The user slides the multivalve (D), closing off the urine suction tube, opening the lysis buffer and urine outlets to the mixer, and providing openings for both interlock rods. In the final step, the user pushes down on the lysis buffer plunger (E), ejecting urine and lysis buffer through a static mixer, wherein the solutions are well mixed before finally being ejected from the tip of the mixer. Red blocks at the bottom of each panel show a top-down view of the multivalve. Black circles and rings indicate holes in the multivalve. Slashed circles indicate the presence of a feature that is blocked by the multivalve. Colored circles indicate the presence of an interlock rod or an open channel for the flow of a solution. Reproduced from [94] with permission from the Royal Society of Chemistry.

Similarly, a microfluidic valve was polyjet printed using a flexible material (TangoPlus) and a stiff material (VeroWhitePlus) for valve actuation and the external valve structures, respectively. Compared with a previously reported single material valve, this multimaterial valve showed stronger resistance of deformation. The valve also showed proportional control over a flow rate ranging from 0 and 50 μL/s without deformation. The application of this valve in DNA assembly and analysis, continuous sampling and sensing, and soft robotics is expected.[95] Jiang *et al*. fabricated a microfluidic device integrated with pneumatic microvalves *via* multimaterial 3D printing using both rigid and flexible materials. This device can be used to precisely control the liquid flow.[96]

3.3.2 Sensors and electronics

Rymansaib and co-wokers 3D printed an electrochemical device using polystyrene and customized carbon nanofiber (CNF)-graphite based polystyrene (PS) with a dual-head FDM printer as shown in Figure 2.8. Firstly the authors optimized the conductive composite material formulations, different base materials including ABS, polycaprolactone (PCL), and PS were blended with CNF and graphite. PS was chosen as the base material as ABS or PCL based composites gave poor voltammetric response probably due to interfacial wetting effects. Then the other non-conductive material was also optimized by comparing PLA, Polypropylene (PP) and PS; PS was the optimal material for shell fabrication as it gave superior conductivity results throughout. Finally the device was used for cyclic voltammetry of aqueous 1,1'-ferrocenedimethanol and differential pulse voltammetry detection of aqueous Pb^{2+} *via* anodic stripping.[53]

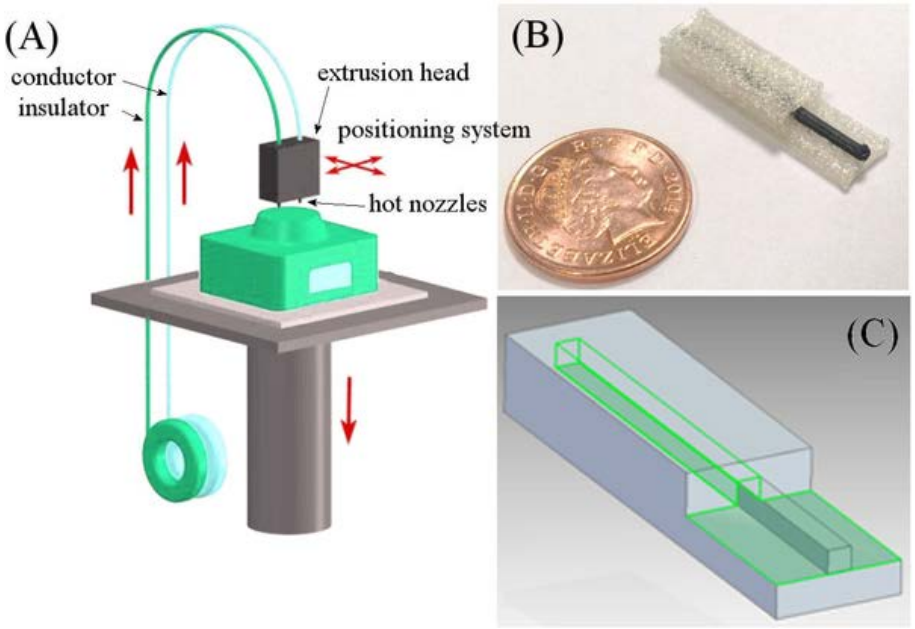

Figure 2.8 (A) Schematic diagram of a 3D printing set up with two feeds (polystyrene insulator and polystyrene composite conductor) being printed through a hot nozzle system with positional controller. (B) Photograph of a printed polystyrene-nanocarbon composite electrode. (C) Multi-part electrode being designed in CAD software. Reproduced from [53] with permission from the WILEY.

Park and co-authors 3D printed a three-layer lithium battery. The anode, electrolyte, and cathode were sequentially printed using different conductive cellulose composites using the combination of a commercial FDM 3D printer and a paste extrusion system to enable simultaneous printing of different parts.[30] Rocha *et al.* 3D printed a graphene based device for electrochemical energy storage. This device was fabricated using an aqueous-based thermoresponsive formulation including a chemically modified graphene (CMG) as the active material and copper as current collector in a single step with an extrusion printer. After printing, the printed device was frozen in liquid nitrogen and freeze-dried for 48 h, followed by thermal reduction at 900 °C for 1 h. Using this device, the specific energy and power densities reached values of 26 Wh kg^{-1} and 13 Kw kg^{-1}, and has a promising and long-term stability.[52] Various functional electronic sensors were 3D printed and integrated with other supported parts using a triple-head FDM printer for sensing mechanical flexing. The electrode was printed with a customized conductive filament (termed 'carbomorph') using one of the nozzles, and the supporting parts were printed using the other two nozzles, thus there was no need to replace the filaments when printing different parts, also allowing the creation of much more complex structures than if the filament needs to be replaced in a single head printer.[54] Phung and co-workers 3D printed a fluidic device with integrated electrodes for isotachophoresis (ITP) of bacterial cells. The device was printed using a dual-head FDM printer, with ABS for fluidic device fabrication and carbon based ABS for electrodes fabrication. The 3D printed electrode had a higher resistance when compared to Pt electrode, which reduced the highest voltages available for electrophoresis, but the authors still successfully used this device for carry on a stable ITP experiment for bacterial cells.[97]

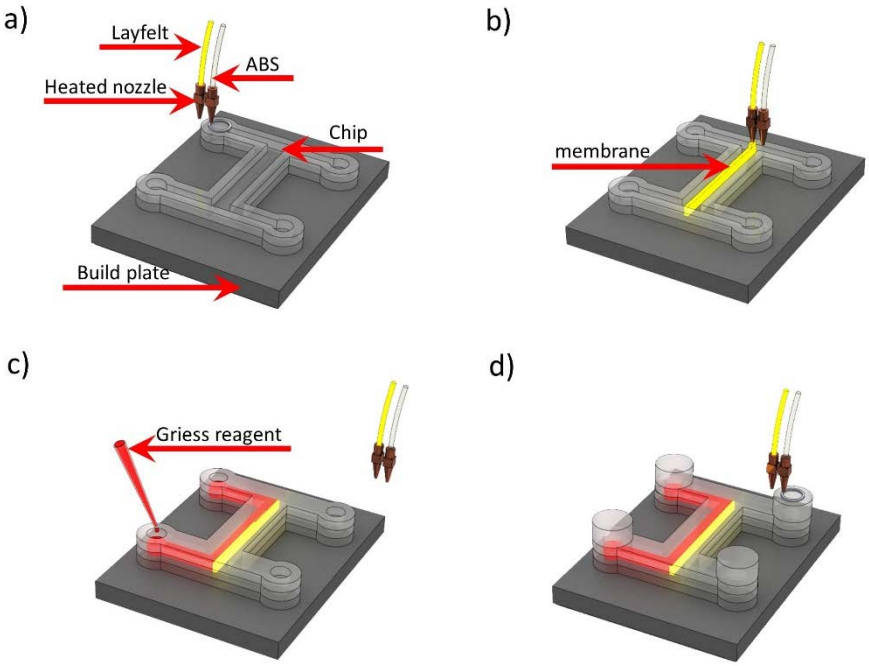

Figure 2.9 Schematic of embedding Griess reagent during 3D printing process. (a) Chip printing with ABS. (b) Membrane printing with Lay-felt. (c) Embedding Griess reagent while pausing the printing process. (d) Continuing printing to seal the reservoir. Reproduced from [27] with permission from the American Chemical Society.

FDM printing allows for the embedding of liquid reagents through PPP during fabrication, a unique capability that is difficult to realize with the same ease using traditional approaches.[27] An impeller flow sensor was fabricated with multimaterial FDM printing, the main body of the sensor was printed with ABS to maintain the structural integrity of the impeller, and a magnetic filament was printed on the top surface of the ABS body to sense the flow rate. The 3D printed flow sensor showed comparable performance with commercial sensor in terms of the linearity of its response and repeatability.[98]

3.3.3 Porous structures and membranes

A multimateial FDM printer was used to fabricate a microfluidic device with a printed integrated membrane by Li *et al*. Liquid reagent was also embedded into the device, as shown in Figure 2.9, making it suitable for the direct analysis of nitrate in soil. The integrated membrane was 3D printed with a commercially available porous composite (Lay-felt), eliminating additional processing steps and maintaining an automated fabrication pathway.[27]

3.3.4 Fluidic interconnects and modular systems

A 3D printed microfluidic device with integrated microdialysis probes for continuous monitoring of glucose and lactate in human tissues was demonstrated. The microfluidic device as well as the holders or threaded ports for electrodes and biosensors integration were 3D printed, the base of the holder was printed using a soft, compressible plastic to ensure the holder made a seal with the microfluidic chip, needle electrodes and in-house wireless potentiostats were then integrated. With this system, monitoring real-time subcutaneous glucose and lactate levels for assessing athlete's performance during sports activities could be achieved.[99] Similarly, a microfluidic chip interconnect composing of clamp and gasket was fabricated *via* multimaterial 3D printing a rigid plastic (VeroBlack®) and a flexible elastomer (TangoBlack®), respectively. This

interconnect showed the ability to withstand pressure above 400 kPa.[100] Lockwood and co-workers 3D printed a fluidic device with an integrated porous membrane-based insert, with wells for in vitro pharmacokinetic profiling of drug molecules. The device containing six flow channels with wells above the channels was printed with a rigid plastic (VeroClear®), with the Fullcure 980 TangoBlackPlus material used to fabricate an O-ring that lined the inside of the wells to create a seal between Transwell inserts and the fluidic device.[101] A 3D printed fluidic device with threaded ports allowed integration of PEEK tubing and electrodes. The fluidic device was printed using polyethylene terephthalate (PET), and threaded fittings were printed with ABS. This device was used to prepare Prussian blue nanoparticles, which were then attached to gold electrodes for hydrogen peroxide sensing, and a limit of detection of 100 nM was achieved.[102]

4. Conclusions

Functionally integrated microfluidic devices allow for miniaturization and automation of the complex workflow required for chemical analysis, combining sample processing and analysis in a single device. Traditional manufacturing methods for integrated microfluidic devices have limitations such as expensive infrastructure, limited flexibility in design, especially 3D, limited choice of materials and combinations thereof and time-intensive processing steps. 3D printing provides solutions to reduce these limitations; particularly for the fabrication of integrated devices. Three approaches can be identified at present: single material 3D printing, PPP 3D printing and multimaterial 3D printing. Single material 3D printing currently dominates the field of integrated device fabrication, and integrated functionalities result from the design and adjustments to printing process to exploit the intrinsic properties of the material. PPP 3D printing has enabled the integration of external components or materials into the 3D printed object, and was used

to incorporate electronics, chemical reagents and membranes. Multimaterial 3D printing combines materials with different properties in a single print, and extrusion based printing (such as FDM) and jetting based printing techniques have been used for manufacturing integrated devices using an automated process. Combinations have included conducting, flexible and porous materials, but to take full advantage of this capability, a larger variety of materials with different physical and chemical properties will be required. Lastly, to lift 3D printing from a prototyping to a manufacturing platform for the production of complex, integrated microfluidic devices at a quality that is competitive with traditional manufacturing platforms, printers with increased resolution and speed will be required.

References

(1) Kilby, J. S.; U.S. Patent, 1964.

(2) Judy, J. W. *Smart materials and Structures* **2001**, *10*, 1115.

(3) Grayson, A. R.; Shawgo, R. S.; Johnson, A. M.; Flynn, N. T.; Li, Y.; Cima, M. J.; Langer, R. *Proceedings of the IEEE* **2004**, *92*, 6-21.

(4) Manz, A.; Graber, N.; Widmer, H. á. *Sensors and actuators B: Chemical* **1990**, *1*, 244-248.

(5) Choi, J.-W.; Oh, K. W.; Thomas, J. H.; Heineman, W. R.; Halsall, H. B.; Nevin, J. H.; Helmicki, A. J.; Henderson, H. T.; Ahn, C. H. *Lab on a Chip* **2002**, *2*, 27-30.

(6) Li, F.; Guijt, R. M.; Breadmore, M. C. *Analytical chemistry* **2016**, *88*, 8257-8263.

(7) Shallan, A. I.; Guijt, R. M.; Breadmore, M. C. *Angewandte Chemie* **2015**, *127*, 7467-7470.

(8) Easley, C. J.; Karlinsey, J. M.; Bienvenue, J. M.; Legendre, L. A.; Roper, M. G.; Feldman, S. H.; Hughes, M. A.; Hewlett, E. L.; Merkel, T. J.; Ferrance, J. P. *Proceedings of the National Academy of Sciences* **2006**, *103*, 19272-19277.

(9) Lagally, E.; Medintz, I.; Mathies, R. *Analytical chemistry* **2001**, *73*, 565-570.

(10) Lagally, E. T.; Simpson, P. C.; Mathies, R. A. *Sensors and Actuators B: Chemical* **2000**, *63*, 138-146.

(11) Wei, H.; Li, H.; Lin, J.-M. *Journal of Chromatography A* **2009**, *1216*, 9134-9142.

(12) Liu, B.; Zhang, Y.; Mayer, D.; Krause, H. J.; Jin, Q.; Zhao, J.; Offenhäusser, A. *Electrophoresis* **2011**, *32*, 699-704.

(13) Broyles, B. S.; Jacobson, S. C.; Ramsey, J. M. *Analytical chemistry* **2003**, *75*, 2761-2767.

(14) Mason, B. P.; Price, K. E.; Steinbacher, J. L.; Bogdan, A. R.; McQuade, D. T. *Chemical reviews* **2007**, *107*, 2300-2318.

(15) Shields IV, C. W.; Reyes, C. D.; López, G. P. *Lab on a Chip* **2015**, *15*, 1230-1249.

(16) Gross, B.; Lockwood, S. Y.; Spence, D. M. *Analytical Chemistry* **2016**, *89*, 57-70.

(17) Jang, J.; Yi, H.-G.; Cho, D.-W. *ACS Biomaterials Science & Engineering* **2016**, *2*, 1722-1731.

(18) Sydney Gladman, A.; Matsumoto, E. A.; Nuzzo, R. G.; Mahadevan, L.; Lewis, J. A. *Nat Mater* **2016**, *advance online publication*.

(19) Waheed, S.; Cabot Canyelles, J.-M.; Macdonald, N.; Guijt, R. M.; Lewis, T.; Paull, B.; Breadmore, M. C. *Lab on a Chip* **2016**, *16*, 1993-2013.

(20) Macdonald, N. P.; Cabot, J. M.; Smejkal, P.; Guijt, R. M.; Paull, B.; Breadmore, M. C. *Analytical Chemistry* **2017**, *89*, 3858-3866.

(21) Shallan, A. I.; Smejkal, P.; Corban, M.; Guijt, R. M.; Breadmore, M. C. *Analytical chemistry* **2014**, *86*, 3124-3130.

(22) Au, A. K.; Huynh, W.; Horowitz, L. F.; Folch, A. *Angewandte Chemie International Edition* **2016**, n/a-n/a.

(23) Bhattacharjee, N.; Urrios, A.; Kang, S.; Folch, A. *Lab on a Chip* **2016**, *16*, 1720-1742.

(24) Macdonald, N. P.; Currivan, S. A.; Tedone, L.; Paull, B. *Analytical chemistry* **2017**.

(25) Symes, M. D.; Kitson, P. J.; Yan, J.; Richmond, C. J.; Cooper, G. J. T.; Bowman, R. W.; Vilbrandt, T.; Cronin, L. *Nat Chem* **2012**, *4*, 349-354.

(26) Su, C.-K.; Peng, P.-J.; Sun, Y.-C. *Analytical chemistry* **2015**, *87*, 6945-6950.

(27) Li, F.; Smejkal, P.; Macdonald, N. P.; Guijt, R. M.; Breadmore, M. C. *Analytical Chemistry* **2017**, *89*, 4701-4707.

(28) Sundaram, S.; Kim, D. S.; Baldo, M. A.; Hayward, R. C.; Matusik, W. *ACS applied materials & interfaces* **2017**, *9*, 32290-32298.

(29) Flowers, P. F.; Reyes, C.; Ye, S.; Kim, M. J.; Wiley, B. J. *Additive Manufacturing* **2017**, *18*, 156-163.

(30) Park, J. S.; Kim, T.; Kim, W. S. *Scientific Reports* **2017**, *7*, 3246.

(31) MacDonald, E.; Wicker, R. *Science* **2016**, *353*, aaf2093.

(32) Melchels, F. P.; Feijen, J.; Grijpma, D. W. *Biomaterials* **2010**, *31*, 6121-6130.

(33) Kolesky, D. B.; Truby, R. L.; Gladman, A.; Busbee, T. A.; Homan, K. A.; Lewis, J. A. *Advanced materials* **2014**, *26*, 3124-3130.

(34) Macdonald, N. P.; Zhu, F.; Hall, C.; Reboud, J.; Crosier, P.; Patton, E.; Wlodkowic, D.; Cooper, J. *Lab on a Chip* **2016**, *16*, 291-297.

(35) Gosselin, C.; Duballet, R.; Roux, P.; Gaudillière, N.; Dirrenberger, J.; Morel, P. *Materials & Design* **2016**, *100*, 102-109.

(36) Kroll, E.; Artzi, D. *Rapid Prototyping Journal* **2011**, *17*, 393-402.

(37) Heo, D. N.; Castro, N. J.; Lee, S.-J.; Noh, H.; Zhu, W.; Zhang, L. G. *Nanoscale* **2017**, *9*, 5055-5062.

(38) Kinstlinger, I. S.; Miller, J. S. *Lab on a Chip* **2016**, *16*, 2025-2043.

(39) Lehner, B. A.; Schmieden, D. T.; Meyer, A. S. *ACS synthetic biology* **2017**, *6*, 1124-1130.

(40) He, Y.; Wu, Y.; Fu, J. z.; Gao, Q.; Qiu, J. j. *Electroanalysis* **2016**, *28*, 1658-1678.

(41) Chya-Yan, L.; Murat, G. *Biofabrication* **2017**, *9*, 024102.

(42) Michalski, M. H.; Ross, J. S. *Jama* **2014**, *312*, 2213-2214.

(43) Rogers, C. I.; Qaderi, K.; Woolley, A. T.; Nordin, G. P. *Biomicrofluidics* **2015**, *9*, 016501.

(44) Au, A. K.; Bhattacharjee, N.; Horowitz, L. F.; Chang, T. C.; Folch, A. *Lab on a Chip* **2015**, *15*, 1934-1941.

(45) Gong, H.; Woolley, A. T.; Nordin, G. P. *Lab on a Chip* **2016**.

(46) Campbell, I.; Bourell, D.; Gibson, I. *Rapid prototyping journal* **2012**, *18*, 255-258.

(47) Mueller, B. *Assembly Automation* **2012**, *32*.

(48) Vaezi, M.; Chianrabutra, S.; Mellor, B.; Yang, S. *Virtual and Physical Prototyping* **2013**, *8*, 19-50.

(49) Chan, H. N.; Tan, M. J. A.; Wu, H. *Lab on a Chip* **2017**.

(50) Scotti, G.; Nilsson, S. M. E.; Haapala, M.; Poho, P.; Boije af Gennas, G.; Yli-Kauhaluoma, J.; Kotiaho, T. *Reaction Chemistry & Engineering* **2017**, *2*, 299-303.

(51) Symes, M. D.; Kitson, P. J.; Yan, J.; Richmond, C. J.; Cooper, G. J.; Bowman, R. W.; Vilbrandt, T.; Cronin, L. *Nature Chemistry* **2012**, *4*, 349-354.

(52) Rocha, V. G.; García-Tuñón, E.; Botas, C.; Markoulidis, F.; Feilden, E.; D'Elia, E.; Ni, N.; Shaffer, M.; Saiz, E. *ACS Applied Materials & Interfaces* **2017**, *9*, 37136-37145.

(53) Rymansaib, Z.; Iravani, P.; Emslie, E.; Medvidović-Kosanović, M.; Sak-Bosnar, M.; Verdejo, R.; Marken, F. *Electroanalysis* **2016**, *28*, 1517-1523.

(54) Leigh, S. J.; Bradley, R. J.; Purssell, C. P.; Billson, D. R.; Hutchins, D. A. *PLOS ONE* **2012**, *7*, e49365.

(55) Xu, Y.; Wu, X.; Guo, X.; Kong, B.; Zhang, M.; Qian, X.; Mi, S.; Sun, W. *Sensors* **2017**, *17*, 1166.

(56) Wang, J.; McMullen, C.; Yao, P.; Jiao, N.; Kim, M.; Kim, J.-W.; Liu, L.; Tung, S. *Microfluidics and Nanofluidics* **2017**, *21*, 105.

(57) Gong, H.; Woolley, A. T.; Nordin, G. P. *Lab on a Chip* **2016**, *16*, 2450-2458.

(58) Macdonald, N. P.; Currivan, S. A.; Tedone, L.; Paull, B. *Analytical chemistry* **2017**, *89*, 2457-2463.

(59) Belka, M.; Ulenberg, S.; Bączek, T. *Analytical Chemistry* **2017**.

(60) Fichou, D.; Morlock, G. E. *Analytical chemistry* **2017**, *89*, 2116-2122.

(61) Norouzi, N.; Bhakta, H. C.; Grover, W. H. *PloS one* **2016**, *11*, e0149259.

(62) Li, F.; Macdonald, N. P.; Guijt, R. M.; Breadmore, M. C. *Analytical chemistry* **2017**, *89*, 12805-12811.

(63) Bhargava, K. C.; Thompson, B.; Malmstadt, N. *Proceedings of the National Academy of Sciences* **2014**, *111*, 15013-15018.

(64) Nie, J.; Gao, Q.; Qiu, J.-j.; Sun, M.; Liu, A.; Shao, L.; Fu, J.; Zhao, P.; He, Y. *Biofabrication* **2018**.

(65) Chan, H. N.; Shu, Y.; Xiong, B.; Chen, Y.; Chen, Y.; Tian, Q.; Michael, S. A.; Shen, B.; Wu, H. *ACS Sensors* **2015**.

(66) Hinsmann, P.; Frank, J.; Svasek, P.; Harasek, M.; Lendl, B. *Lab on a Chip* **2001**, *1*, 16-21.

(67) Song, Y.; Hormes, J.; Kumar, C. S. *small* **2008**, *4*, 698-711.

(68) Pihl, J.; Sinclair, J.; Sahlin, E.; Karlsson, M.; Petterson, F.; Olofsson, J.; Orwar, O. *Analytical Chemistry* **2005**, *77*, 3897-3903.

(69) Seong, G. H.; Crooks, R. M. *Journal of the American Chemical Society* **2002**, *124*, 13360-13361.

(70) Stroock, A. D.; Dertinger, S. K.; Ajdari, A.; Mezić, I.; Stone, H. A.; Whitesides, G. M. *Science* **2002**, *295*, 647-651.

(71) Plevniak, K.; Campbell, M.; Myers, T.; Hodges, A.; He, M. *Biomicrofluidics* **2016**, *10*, 054113.

(72) Carrière, P. *Physics of fluids* **2007**, *19*, 118110.

(73) Cabot, J. M.; Fuguet, E.; Roses, M.; Smejkal, P.; Breadmore, M. C. *Analytical chemistry* **2015**, *87*, 6165-6172.

(74) Liao, Y.; Song, J.; Li, E.; Luo, Y.; Shen, Y.; Chen, D.; Cheng, Y.; Xu, Z.; Sugioka, K.; Midorikawa, K. *Lab on a Chip* **2012**, *12*, 746-749.

(75) Macdonald, N. P.; Cabot, J. M.; Smejkal, P.; Guijt, R. M.; Paull, B.; Breadmore, M. C. *Analytical chemistry* **2017**, *89*, 3858-3866.

(76) Lee, K. G.; Park, K. J.; Seok, S.; Shin, S.; Park, J. Y.; Heo, Y. S.; Lee, S. J.; Lee, T. J. *RSC Advances* **2014**, *4*, 32876-32880.

(77) Yuen, P. K. *Lab on a Chip* **2008**, *8*, 1374-1378.

(78) Yuen, P. K. *Lab on a Chip* **2016**, *16*, 3700-3707.

(79) Yuen, P. K.; Bliss, J. T.; Thompson, C. C.; Peterson, R. C. *Lab on a Chip* **2009**, *9*, 3303-3305.

(80) MacDonald, E.; Wicker, R. *Science* **2016**, *353*.

(81) Duarte, L. C.; Chagas, C. L. S.; Ribeiro, L. E. B.; Coltro, W. K. T. *Sensors and Actuators B: Chemical* **2017**, *251*, 427-432.

(82) Gaal, G.; Mendes, M.; de Almeida, T. P.; Piazzetta, M. H. O.; Gobbi, Â. L.; Riul Jr, A.; Rodrigues, V. *Sensors and Actuators B: Chemical* **2017**, *242*, 35-40.

(83) Banna, M.; Bera, K.; Sochol, R.; Lin, L.; Najjaran, H.; Sadiq, R.; Hoorfar, M. *Sensors* **2017**, *17*, 1336.

(84) Kitson, P. J.; Marshall, R. J.; Long, D.; Forgan, R. S.; Cronin, L. *Angewandte Chemie International Edition* **2014**, *53*, 12723-12728.

(85) Kitson, P. J.; Symes, M. D.; Dragone, V.; Cronin, L. *Chemical Science* **2013**, *4*, 3099-3103.

(86) Kitson, P. J.; Rosnes, M. H.; Sans, V.; Dragone, V.; Cronin, L. *Lab on a Chip* **2012**, *12*, 3267-3271.

(87) Yuen, P. K. *Biomicrofluidics* **2016**, *10*, 044104.

(88) Pinger, C.; Heller, A.; Spence, D. M. *Analytical Chemistry* **2017**, *89*, 7302-7306.

(89) Lederle, F.; Meyer, F.; Kaldun, C.; Namyslo, J. C.; Hübner, E. G. *New Journal of Chemistry* **2017**, *41*, 1925-1932.

(90) Choi, J.-W.; Kim, H.-C.; Wicker, R. *Journal of Materials Processing Technology* **2011**, *211*, 318-328.

(91) Visser, J.; Peters, B.; Burger, T. J.; Boomstra, J.; Dhert, W. J.; Melchels, F. P.; Malda, J. *Biofabrication* **2013**, *5*, 035007.

(92) Murphy, S. V.; Atala, A. *Nature biotechnology* **2014**, *32*, 773.

(93) Begolo, S.; Zhukov, D. V.; Selck, D. A.; Li, L.; Ismagilov, R. F. *Lab on a Chip* **2014**, *14*, 4616-4628.

(94) Jue, E.; Schoepp, N. G.; Witters, D.; Ismagilov, R. F. *Lab on a Chip* **2016**, *16*, 1852-1860.

(95) Keating, S. J.; Gariboldi, M. I.; Patrick, W. G.; Sharma, S.; Kong, D. S.; Oxman, N. *PLoS ONE* **2016**, *11*.

(96) Jiang, X.; Lillehoj, P. B. In *Nano/Micro Engineered and Molecular Systems (NEMS), 2017 IEEE 12th International Conference on*; IEEE, 2017, pp 38-41.

(97) Phung, S.; Li, F.; Macka, M.; Guijt, S. P. R.; Breadmore, M. In *20th International Conference on Miniaturized Systems for Chemistry and Life Sciences, MicroTAS 2016*, 2016, pp 1081-1082.

(98) Leigh, S. J.; Purssell, C. P.; Billson, D. R.; Hutchins, D. A. *Smart Materials and Structures* **2014**, *23*, 095039.

(99) Gowers, S. A.; Curto, V. F.; Seneci, C. A.; Wang, C.; Anastasova, S.; Vadgama, P.; Yang, G.-Z.; Boutelle, M. G. *Analytical chemistry* **2015**, *87*, 7763-7770.

(100) Paydar, O.; Paredes, C.; Hwang, Y.; Paz, J.; Shah, N.; Candler, R. *Sensors and Actuators A: Physical* **2014**, *205*, 199-203.

(101) Lockwood, S. Y.; Meisel, J. E.; Monsma, F. J.; Spence, D. M. *Analytical Chemistry* **2016**.

(102) Bishop, G. W.; Satterwhite, J.; Bhakta, S.; Kadimisetty, K.; Gillette, K. M.; Chen, E.; Rusling, J. F. *Analytical chemistry* **2015**.

Table 1. 3D printed integrated device

Integrating approaches	Integrated functionalities	Application	3D printing technology	Print materials	Reference
Single material 3D printing	Pump, mixer	Chemiluminescence immunoassay of insulin	FDM	Flexible TPE	56
	Valve	Microfluidic valve for fluid control	SLA	Customized resin	43
	Valve, pump, mixer	Fluid control	SLA	Customized resin	57
	Valve, pump	Cell culture applications	SLA	WaterShed XC 11122 resin	44
	Valve, pump	Colorimetric analysis of proteins in urine	SLA	BV-003 resin	65
	Mixer	Colorimetric detection of blood haemoglobin level	PolyJet	VisiJetV® FTX Clear resin	71
	Mixer	Mixing of two dyes	SLA	BV-001 resin	21
	Mixer	Automated pKa determination	SLA	BV-001 resin	73
	Mixer	Extraction of trace elements in seawater	SLA	BV-001 resin	26
	Mixer	Fluid mixing	DLW	Glass	74
	Mixer	Fluid control in microfluidics	FDM, SLA, PolyJet	ABS, BV-007 resin, Veroclear-RGD810	75
	Mixer	Colorimetric analysis of Fe^{3+} in water	FDM	ABS	62
	Mixer	Fluid mixing control	SLA	UV cured Resin	61
	Porous structures	TLC separation different dyes	Modified FDM	Silica gel	60
	Porous structures	TLC separation different preotiens	PolyJet	Veroclear-RGD810	58
	Porous structures	Extraction of drugs from water	FDM	LAY-FOMM 60	59
	Modular microfluidics	Microdroplet generator	SLA	Somos WaterShed XC 11122 photoresin	63

	Modular microfluidics	"SmartBuild System" for biological and chemical applications	SLA	UV cured Resin	77
	Modular microfluidics	Reconfigurable stick-n-play microfluidic system	FDM	XT Copolyester Filament	78
	Modular microfluidics	Multidimensional microfluidic systems	SLA	UV cured Resin	79
	Modular microfluidics	Detection of AFP biomarker	PolyJet	VisiJet M3 Crystal	76
Print-pause-print 3D printing	Electronics	Measuring the size of microdroplets *via* capacitively coupled contactless conductivity detection (C4D) detection	FDM	CNT-doped PLA	81
	Electronics	Electronic tongue	FDM	PLA	82
	Electronics	pH and conductivity sensing for water monitoring	FDM	ABS	83
	Chemical reactants	3D printed reaction ware with printed catalyst chemical synthesis	FDM	PP	84-86
	Chemical reactants	3D printed reactor for online mass spectrometry monitoring of the chemical reaction	FDM	PP	50
	Chemical reactants	Synthesis of arylnaphthylalkynes with NMR spectroscopy	FDM	Polyamide	89
	Membrane	3D printed device for continuous perfusion cell culturing	FDM	XT Copolyester Filament	87
	Membrane	3D printed equilibrium-dialysis device for investigating the binding of small molecules and ions to proteins	PolyJet	VeroClear	88
Multimaterial 3D printing	Pump	3D printed pumping lid for controlling flow in droplet microfluidics and sample loading	PolyJet	VeroClear, TangoBlack	93
	Pump	3D printed interlock meter-mix device for accurately sample metering	PolyJet	VeroClear, TangoBlack	94

	Valve	Microfluidic valve	PolyJet	VeroWhitePlus, TangoBlack	95
	Valve	Pneumatic microvalves	PolyJet	VeroClear, TangoBlack	96
	Interconnect	Monitoring real-time subcutaneous glucose and lactate levels	PolyJet	VeroWhitePlus, TangoBlack	99
	Interconnect	3D-printed microfluidic chip with interconnects	PolyJet	VeroBlack, TangoBlack	100
	Interconnect	3D printed diffusion based device for in vitro pharmacokinetic study	PolyJet	VeroClear, TangoBlack	101
	Interconnect	Amperometric detection of H2O2	FDM	ABS, PET	102
	Electronics	Voltammetric sensing of heavy metals in water	FDM	Polystyrene, conductive filament	53
	Electronics	3D printed lithium battery	Modified FDM	Customized materials	30
	Electronics	Electrochemical energy storage	Modified FDM	Copper and graphene	52
	Electronics	3D printed electronic sensors for sensing mechanical flexing	FDM	Carbon Black contained filament, PLA	54
	Electronics	ITP of bacterial	FDM	ABS, cabon doped ABS	97
	Membrane	Direct soil nitrate detection	FDM	ABS, LAY-FELT	27
	Magnet	3D printed impeller flow sensor	FDM	Magnet filament, ABS	98

Chapter 3 has been removed for copyright or proprietary reasons.

It has been published as: Li, F., Guijt, R. M., Breadmore, M. C., 2016. Nanoporous membranes for microfluidic concentration prior to electrophoretic separation of proteins in urine, Analytical chemistry, 88(16), 8257-8263

Chapter 4 has been removed for copyright or proprietary reasons.

It has been published as: Li, F., Smejkel, P., Macdonald, N. P., Guijt, R. M., Breadmore, M. C., 2017. One-step fabrication of a microfluidic device with an integrated membrane and embedded reagents by multimaterial 3D printing, Analytical chemistry, 89(8), 4701-4707

Chapter 5 has been removed for copyright or proprietary reasons.

It has been published as: Li, F., Macdonald, N. P., Guijt, R. M., Breadmore, M. C., 2017. Using printing orientation for tuning fluidic behavior in microfluidic chips made by fused deposition modeling 3D printing, 89(23), 12805-12811

3D Printing clinical diagnostic devices

Feng Li,[1,2] Niall P. Macdonald,[1,2] Rosanne M. Guijt,[3] and Michael C. Breadmore[1,2*]

[1] Australian Centre for Research on Separation Science, School of Chemistry, University of Tasmania, Private Bag 75, Hobart, Tasmania 7001, Australia

[2] ARC Centre of Excellence for Electromaterials Science (ACES), School of Chemistry, University of Tasmania, Private Bag 75, Hobart, Tasmania 7001, Australia

[3] Centre for Rural and Regional Futures, Deakin University, Geelong, Private Bag 20000, 3220 Geelong, Australia

Abstract

Multimaterial 3D printing provides a unique capability for the creation of highly complex integrated devices where complementary functionality is realized using differences in material properties. Using a single and automated print process, microfluidic devices can be fabricated containing (i) an optically transparent structure for inspection and detection, (ii) electrodes for electrokinetic transport, (iii) a primary membrane to remove particulates and macromolecules including proteins, and (iv) a secondary membrane to concentrate small molecule targets. The device was used for the extraction and concentration of small molecule pharmaceuticals from urine, combined with on-chip electrophoretic separation of concentrated targets for quantitative analysis. Owing to the high level of functional integration inside the device, manual handling is minimal and restricted to the introduction of the sample and buffer solutions. The 3D printed sample-in/answer-out device allows for the direct quantification a model pharmaceutical, ampicillin, in untreated urine within 3 min, down to 2 ppm.

* Michael.Breadmore@utas.edu.au

These results demonstrate the potential of 3D printing for on-demand fabrication of disposable, functionally integrated devices for low-cost point-of-collection (POC) diagnostics.

POC testing requires the ability to detect and quantify analytical target(s) directly from a complex sample without user intervention. The field is dominated by tests that exploit the exquisite selectivity of antibodies and/or enzymes, however for small molecule targets, such as many biomarklers, pharmaceuticals and their metabolites, cross-selectivity may lead to inaccurate results. Larger, laboratory-housed instrumentation, such as chromatographs and mass spectrometers can be used to accurately quantify these molecules. The next evolution of POCT devices is the miniaturization and translation of this instrumentation into small portable devices to provide this accuracy at the point of sample collection. This concept, first discussed in the late 80's, has been proven difficult to realise because of the technical difficulty in fabricating devices capable of accomodating complex and disparate chemical processes in a simple, affordable and automated manner. For example, a typical workflow for the analysis of pharmaceuticals from blood/serum/plasma in a laboratory setting requires extraction of the targets from the sample, frequently involving a volume reduction step, followed by separation on a liquid chromatograph with mass spectrometry detection. An integrated device for POC testing must contain all of the structures, materials and reagents for a similar but automated workflow.

Currently the most cost-effective approach to manufacture microfluidic devices is using mass-replication techniques, such as injection moulding or hot

embossing, as these allow for the thousands of polymeric devices a day. However, the incorporation of different materials and reagents needed for the functionality described above significantly increases the cost of each device. For example, a membranes can be integrated by positioning it on top of one substrate and sealing it in place by bonding with the second substrate.[1,2]. The associated additional processing increases the cost per device from €20 (100+) each to €45 each (100+). The integration of electrodes for detection or electrokinetic manipulation increases the costs more significantly, with the cost of electrophoresis chips increasing from €10 each (1000+) to €125 each (30+). The increased cost, which does not reduce considerably with scale, is due to the complexity and laborious nature of positioning metal electrodes in direct contact with the fluids in such a way that the fluidic movement is not impacted, and inspection of each device during quality control. Guijt and co-workers reported electrodes buried in a trench etched by reactive ion etching, and partially covered with a silicon nitrite layer (or silicon carbide when a insulating dielectric medium was required) to yield a planar surface for leakage-free sealing of the microchannel[3].

In this paper, a multimaterial 3D printer is used to create a complex, functionally integrated device for the quantification of pharmaceuticals in blood. 3D printing, or additive manufacturing, allows the precise deposition of materials in a complex 3D geometry to create miniaturized analytical devices.[4-11] Photopolymer inkjet printing and fused deposition modelling (FDM) provide the capability to print two or more different materials in a single print run. Using a combination of flexible materials and rigid materials, Begolo and co-workers fabricated a microfluidic pump using compression of the soft material for

controlled generation of pressure.[12] Inkjet printers have the ability to print upto 5 different materials in a single run, however, the material selection is currently primarily focused on color, and aside from the flexible materials, materials with other physical or chemical properties are not available yet.

For printing microfluidic devices, one of the major limitations of inkjet printers for microfluidics is the difficulty in removing the support material.[13] FDM does not require a support material and because it is not constrained by the use of proprietary materials, a variety of materials available including porous materials,[14,15] conductive filaments,[16,17] flexible filaments,[18,19] ceramic filaments,[20] photonic filaments,[21,22] and drug-containing filaments.[23,24]. Here, we present an integrated microfluidic device comprising of 4 materials printed using a 5-head FDM printer (Figure 1). It contains two membranes of different pore size to create an electrokinetic size and mobility trap[25]. The first membrane (Layfelt™) serves as barrier for electro-extraction, preventing the transport of proteins, cells and particulates (Figure S1, first column) while allowing for the the movement of small molecules and inorganic ions. The second membrane (Laygel™) serves as concentrator, focusing fluorescein by blocking its transport while allowing for the movement of smaller inorganic ions (Figure S1, second column). Thus, the targets are extracted away from the matrix in the sample chamber into the main channel where they are concentrated because they cannot pass through the second membrane. At the end of the extraction/concentration/purification, the fields are switched such that the target molecules migrate down the main channel towards the LE reservoir. The use of a discontinuous electrolyte system allows for separation of the analytes inbto separate zones based on their electrophoretic mobility before passing the

detector. The process is illustrated in Figure 2 using fluorescein as a model analyte. By applying a potential difference of 1000V between the sample and waste channels, the fluorescein intensity in the main channel reaches a similar level to that in the the sample compartment after 100 s (panels a-c), but has been extracted from most matrix components including proteins and particulate matter by the first membrane, while small inorganic ions like chloride have been removed through the second membrane. When the applied potentials are switched to initiate the isotachophoretic separation, the fluorescein is focused into a sharp band with its intensity approximately 5 times higher than the original sample. Figure 3a shows an image and isotachopherogram following the injection of a mixture of fluorescein and ROX, demonstrating their separation into adjacent ITP zones. The 3D printed membrane device was compared with a 3D printed conventional electrophoresis device with more conventionally used pinching and pullback injection (Figure 3b). From the electropherograms, the separation efficiency in the membrane device was similar to that obtained using pinched injection, and it provided a 3-5 fold enhancement in signal, while also purifying the sample.

To demonstrate the applicability of the 3D printed device to perform a complex and authentic assay, the detection of ampicillin from urine is demonstrated. Ampicillin is an antibiotic used to treat bacterial infections, such as respiratory tract infections, urinary tract infections.[26,27] Ampicillin is dosed orally and demonstrates time-dependent killing, where the duration time of free concentration maintained above the minimum inhibitory concentration (MIC) correlates positively with bacterial killing ability.[28] Some side effects of ampicillin such as diarrhea, rash, nausea, etc have been reported when the

concentration is too high.[29] So it is of great importance to ensure the level of ampicillin in biological fluids to ensure it is above the MIC for extended periods of time without over-dosing to mitigate the adverse effects.[30] Urine ampicillin has been detected using HPLC, but all those methods require extensive sample pretreatment such as extraction, purification, and preconcentration before analysis.[30-32]

For analysis using the 3D printed microdevice, a small aliquot of fluorescamine was added to urine samples (both spiked and non-spiked) from a healthy volunteer. Flurorescamine reacts quickly with primary amines like ampicillin present in the urine, to yield a negatively charged, fluorescently labeled compound, whereas the excess fluorescamine loses its fluorescent properties due to hydrolysis. Using the protocol described for fluorescein and ROX, labeled compounds capable of passing the first membrane could be trapped in the main channel between the two membranes before ITP separation. In addition to ampicillin, these include other primary amines present in urine, like amino acids and small peptides. The ITP separation is used to separate the fluorescently labveled ampicillin away from these interferences. As shown in Figure 4, the ampicillin peak is well separated from the other labeled compounds concentrated in the trap. The linear range of 0-100 ppm ampicillin (relative standard deviation (RSD)=21%, n=3 devices, 25 ppm ampicillin) covers the urine level measured using other methods.[30,31,33] The small sample volume (10 μL) and limited sample handling demonstrate the potential of for direct quantitative analysis of pharmaceuticals from body fluids.

The significance of this work is the demonstrated ability to fabricate a device capable of performing a protocol similar to a complex laboratory workflow on

devices fabricated in an automated manner using a single 3D printer. The cost of the 3D printer was less than US $5,000, and the combined material cost for the 4 different materials used to create the device is less than $0.2. This infrastructure and material cost is significantly lower than that associated with conventional microfabrication approaches, especially considering the level of functional integration (2 different membranes and electrodes). With 3D printers anticipated to be widely accessible around the world, this advance will allow for on-demand and on-site fabrication of complex diagnostic devices, with reagents and hardware to be supplied in a kit-like manner. Recognising there are significant technical and regulatory issues that remain to be solved before this will eventuate, the device presented here represents an important step towards low-cost, at-home on-demand production of highly complex devices for advanced chemical analysis in POC settings around the world.

Acknowledgments

F.L. acknowledges the University of Tasmania for the provision of a scholarship. M.C.B. acknowledges an Australian Research Council Future Fellowship Award (FT130100101). R.M.G. acknowledges the Alexander von Humboldt Foundation for the award of a fellowship for Experienced Researchers. Support from the ARC Centre of Excellence for electromaterials Science (ACES; Grant CE140100012) for funding is also acknowledged.

References

(1) Li, F.; Guijt, R. M.; Breadmore, M. C. *Analytical Chemistry* **2016**, *88*, 8257-8263.

(2) Cannon, D. M.; Kuo, T.-C.; Bohn, P. W.; Sweedler, J. V. *Analytical chemistry* **2003**, *75*, 2224-2230.

(3) Guijt, R. M.; Baltussen, E.; van der Steen, G.; Schasfoort, R. B.; Schlautmann, S.; Billiet, H. A.; Frank, J.; van Dedem, G. W.; van den Berg, A. *Electrophoresis* **2001**, *22*, 235-241.

(4) Bhargava, K. C.; Thompson, B.; Malmstadt, N. *Proceedings of the National Academy of Sciences* **2014**, *111*, 15013-15018.

(5) Shallan, A. I.; Smejkal, P.; Corban, M.; Guijt, R. M.; Breadmore, M. C. *Analytical chemistry* **2014**, *86*, 3124-3130.

(6) Cabot, J. M.; Fuguet, E.; Roses, M.; Smejkal, P.; Breadmore, M. C. *Analytical chemistry* **2015**, *87*, 6165-6172.

(7) Kitson, P. J.; Rosnes, M. H.; Sans, V.; Dragone, V.; Cronin, L. *Lab on a Chip* **2012**, *12*, 3267-3271.

(8) Krejcova, L.; Nejdl, L.; Rodrigo, M. A. M.; Zurek, M.; Matousek, M.; Hynek, D.; Zitka, O.; Kopel, P.; Adam, V.; Kizek, R. *Biosensors and Bioelectronics* **2014**, *54*, 421-427.

(9) Erkal, J. L.; Selimovic, A.; Gross, B. C.; Lockwood, S. Y.; Walton, E. L.; McNamara, S.; Martin, R. S.; Spence, D. M. *Lab on a Chip* **2014**, *14*, 2023-2032.

(10) Anderson, K. B.; Lockwood, S. Y.; Martin, R. S.; Spence, D. M. *Analytical chemistry* **2013**, *85*, 5622-5626.

(11) Macdonald, N. P.; Currivan, S. A.; Tedone, L.; Paull, B. *Analytical Chemistry* **2017**, *89*, 2457-2463.

(12) Begolo, S.; Zhukov, D. V.; Selck, D. A.; Li, L.; Ismagilov, R. F. *Lab on a Chip* **2014**, *14*, 4616-4628.

(13) Macdonald, N. P.; Cabot, J. M.; Smejkal, P.; Guijt, R. M.; Paull, B.; Breadmore, M. C. *Analytical Chemistry* **2017**, *89*, 3858-3866.

(14) Li, F.; Smejkal, P.; Macdonald, N. P.; Guijt, R. M.; Breadmore, M. C. *Analytical Chemistry* **2017**, *89*, 4701-4707.

(15) Belka, M.; Ulenberg, S.; Bączek, T. *Analytical Chemistry* **2017**, *89*, 4373-4376.

(16) Gaal, G.; Mendes, M.; de Almeida, T. P.; Piazzetta, M. H. O.; Gobbi, Â. L.; Riul Jr, A.; Rodrigues, V. *Sensors and Actuators B: Chemical* **2017**, *242*, 35-40.

(17) Leigh, S. J.; Bradley, R. J.; Purssell, C. P.; Billson, D. R.; Hutchins, D. A. *PLOS ONE* **2012**, *7*, e49365.

(18) Melnikova, R.; Ehrmann, A.; Finsterbusch, K. In *IOP Conference Series: Materials Science and Engineering*; IOP Publishing, 2014, p 012018.

(19) Sabantina, L.; Kinzel, F.; Ehrmann, A.; Finsterbusch, K. *IOP Conference Series: Materials Science and Engineering* **2015**, *87*, 012005.

(20) Jafari, M.; Han, W.; Mohammadi, F.; Safari, A.; Danforth, S.; Langrana, N. *Rapid Prototyping Journal* **2000**, *6*, 161-175.

(21) Pilleux, M. E.; Safari, A.; Allahverdi, M.; Chen, Y.; Lu, Y.; Jafari, M. A. *Rapid Prototyping Journal* **2002**, *8*, 46-52.

(22) Allahverdi, M.; Danforth, S.; Jafari, M.; Safari, A. *Journal of the European Ceramic Society* **2001**, *21*, 1485-1490.

(23) Goyanes, A.; Wang, J.; Buanz, A.; Martínez-Pacheco, R.; Telford, R.; Gaisford, S.; Basit, A. W. *Molecular Pharmaceutics* **2015**, *12*, 4077-4084.

(24) Goyanes, A.; Chang, H.; Sedough, D.; Hatton, G. B.; Wang, J.; Buanz, A.; Gaisford, S.; Basit, A. W. *International Journal of Pharmaceutics* **2015**, *496*, 414-420.

(25) Shallan, A. I.; Guijt, R. M.; Breadmore, M. C. *Angew. Chem.* **2015**, *54*, 7359-7362.

(26) Stamm, W. E.; Hooton, T. M. *New England journal of medicine* **1993**, *329*, 1328-1334.

(27) Wollschlager, C.; Raoof, S.; Khan, F.; Guarneri, J.; LaBombardi, V.; Afzal, Q. *The American journal of medicine* **1987**, *82*, 164-168.

(28) Adnan, S.; Paterson, D. L.; Lipman, J.; Roberts, J. A. *International journal of antimicrobial agents* **2013**, *42*, 384-389.

(29) Cunha, B. A. *medical Clinics of north america* **2001**, *85*, 149-185.

(30) Parker, S. L.; Adnan, S.; Ordóñez Meija, J. L.; Paterson, D. L.; Lipman, J.; Roberts, J. A.; Wallis, S. C. *Bioanalysis* **2015**, *7*, 2311-2319.

(31) Mišić, I. R.; Miletić, G.; Mitić, S.; Mitić, M.; Pecev-Marinković, E. *Chemical and Pharmaceutical Bulletin* **2013**, *61*, 913-919.

(32) Ibrahim, E.-S. A.; Abdel-Hamid, M.; Abuirjeie, M.; Hurani, A. *Analytical letters* **1988**, *21*, 423-434.

(33) Shrivas, K.; Sahu, J.; Maji, P.; Sinha, D. *New Journal of Chemistry* **2017**, *41*, 6685-6692.

Supporting information

Materials and Chemicals. The FDM filaments (1.75 mm clear ABS, conductive PLA, Lay-Felt, and Lay-Gel) were purchased from MatterHackers Inc. (Foothill Ranch, CA). Bovine serum albumin (BSA), fluorescein sodium salt, fluorescamine, ampicillin, 5(6)-carboxy-X-rhodamine (ROX), ferric chloride ($FeCl_3$), potassium thiocynate (KSCN), Bis-tris (hydroxymethyl) aminomethane (Bis-Tris), 4-(2-hydroxyethyl)-1-piperazineethanesulfonic acid (HEPES), hydrochloric acid (HCl) and polyvinylpyrrolidone (PVP) (Mw=1,300 kDa) were purchased from Sigma-Aldrich Co (Missouri, USA). All solutions were prepared in Milli-Q water obtained from a Millipore (North Ryde, Australia) purification system.

Device design and fabrication. The design of the microfluidic device with membranes and electrodes was accomplished using "AutoCAD 2016 (Student version)" software (Autodesk Inventor, San Rafael, California). Slicing of .stl files into G-code for the ROVA was completed using Simplify3D (www.simplify3d.com), and printing was controlled by Pronterface (www.pronterface.com). The device was printed using a ROVA 3D FDM printer with 5 extruders (ORD Solutions, Canada). The dimensions of the microfluidic channels in ABS were 0.8 × 0.5 mm in width and height, the main channel was 60 mm long, and the Lay-Felt and Lay-Gel membranes were printed to be 0.5 × 1.1 × 5 mm. Before use, the membranes were washed with mili-Q water using a Havard 2000 syringe pump (Harvard Apparatus, Holliston, MA) to dissolve the soluble component from the extruded filament, leaving behind the nanoporous membrane.

Electrokinetic Process. When investigating the size selective transport of Lay-Felt and Lay-Gel membranes, 25/12.5 mM Bis-Tris/HCl buffer (pH 8.5) was used.

Fluorescamine labeled BSA and fluorescein solutions were prepared in Bis-Tris/HCl buffer with a concentration of 20 ppm, 100 ppm $FeCl_3$ and KSCN solutions were prepared in mili-Q water. A chip geometry similar to the one described in our previous paper was used.[14] For the BSA and fluorescein experiments, one channel was filled with sample, and the other channel with buffer. The $FeCl_3$ and KSCN solutions were injected into the respective channels to study Fe^{3+} and SCN^- transport. A 200 V potential difference was applied across the membrane, and an inverted fluorescence microscope (Ti–U, Nikon, Tokyo, Japan) with Nikon high-definition color charge coupled device (CCD) camera (Digital Sight DS-Fi1c, Nikon, Japan) was used to record the migration, as shown in Figure S1.

For all ITP experiments, the leading electrolyte (LE) was 25/12.5 mM Bis-Tris/HCl (pH 8.5) with 1.0% PVP, and the terminating electrolyte (TE) was 10/5 mM Bis-Tris/HEPES (pH 8.0) with 1.0% PVP. As shown in Figure 2, the sample channel and reservoirs (west, W) were filled with fluorescein or mixture of fluorescein and ROX, the waste channel and reservoirs (east, E) were filled with TE, the separation channel and outlet reservoir (south, S) were filled with LE, while the inlet reservoir (north, N) was filled with TE. The applied voltages for extraction were -60, +500, -100, -500 V for 100 s and for ITP -700, +40, +700, +40 V or 200 s at N, E, S and W reservoirs respectively, as shown in Figure 2. For the comparison with pinched injection, all channels were filled with LE, the N and E reservoirs were filled with TE, the S reservoir was filled with LE, and W reservoir was filled with sample. Applied voltages for injection and ITP separation were the same as that of the membrane device. An in-house 4-channel (0–5 kV) DC power supply was used to apply the indicated electrical

potentials to the reservoirs. For the ITP experiments, a USB microscope AM4113T-GFBW (Dino-Lite Premier, Clarkson, WA, Australia) fitted with a blue light-emitting diode for excitation and a 510 nm emission filter was used to record fluorescent images and videos. The microscope objective was fixed at 35X and focused adjusted by changing the distance between the cip and microscope. The image processing software ImageJ (National Institutes of Health, http://rsb.info.nih.gov/ij/) was used to analyze the region of interest (ROI), determining the mean fluorescence intensity in the ROI over time for obtaining the isotachopherograms. The signal intensity of the dark background was valued at 0.

Figure legend

Figure 1. CAD design (a) of chip and 3D printed chip (b).

Figure 2. Fluorescence micrographs captured during extraction (top a, 0s; b, 40s; c, 100s) and ITP preconcentration (bottom d, 20s; e, 100s; f, 200s) of a 2.5 ppm fluorescein. The horizontal blue lines represent the position of the middle channel. The leading electrolyte (LE) was 25/12.5 mM Bis-Tris/HCl (pH 8.5) with 1.0% PVP, and the terminating electrolyte (TE) was 10/5 mM Bis-Tris/HEPES (pH 8.0) with 1.0% PVP.

Figure 3. Electroherograms comparing the 3DP dual membrane device (a) with pinching injection (b) of a mixture of 2.5 ppm fluorescein, 20 ppm 5,6-ROX. The leading electrolyte (LE) was 25/12.5 mM Bis-Tris/HCl (pH 8.5) with 1.0% PVP, and the terminating electrolyte (TE) was 10/5 mM Bis-Tris/HEPES (pH 8.0) with 1.0% PVP.

Figure 4. Analysis of ampicillin in urine. a) Electropherograms for blank urine (bottom) and urine spiked with 50 ppm ampicillin (top). b) The linear calibration curve for ampicillin in urine. The leading electrolyte (LE) was 25/12.5 mM Bis-Tris/HCl (pH 8.5) with 1.0% PVP, and the terminating electrolyte (TE) was 10/5 mM Bis-Tris/HEPES (pH 8.0) with 1.0% PVP.

Figure S1. Size selective permeability for inorganic ions (Fe^{3+}, SCN^-), fluorescein, and fluorescamine labeled BSA for the Layfelt and Laygel membranes. The BGE

was 25/12.5 mM Bis-Tris/HCl buffer, pH was 8.5, a potential difference of 200 V was applied from t = 0 s.

Figure 1

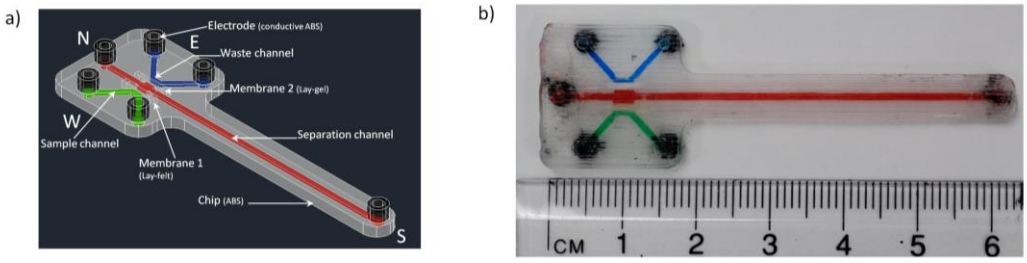

Figure 2

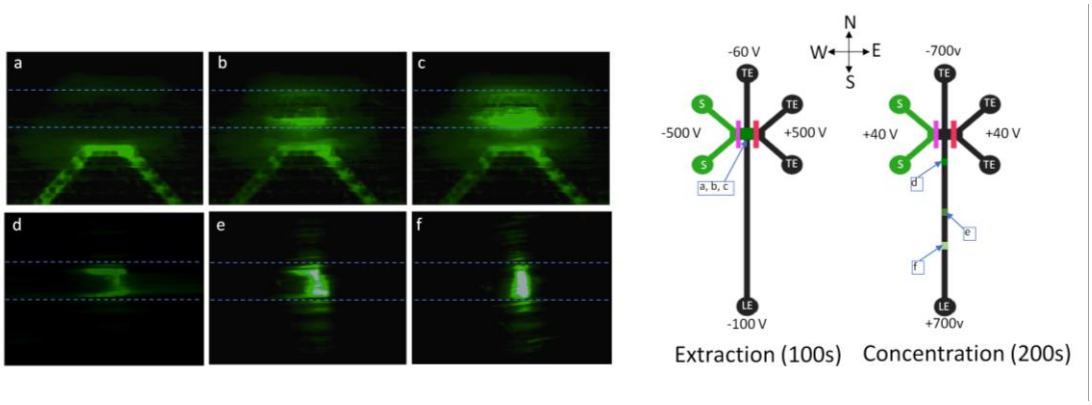

Figure 3

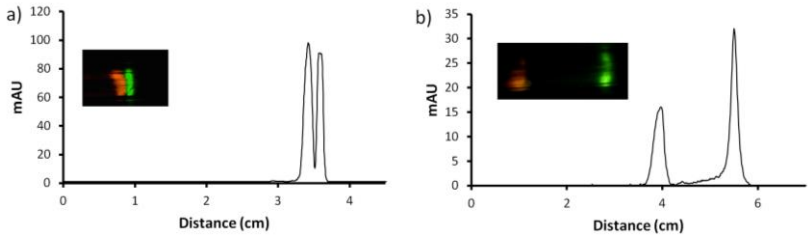

Figure 4

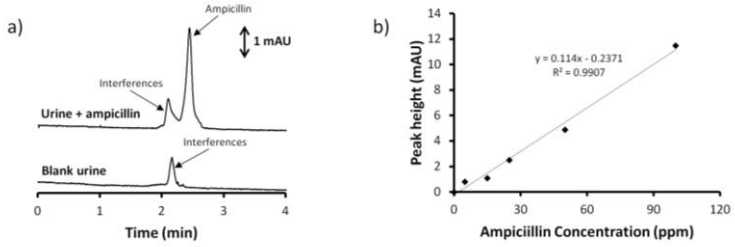

Figure S1

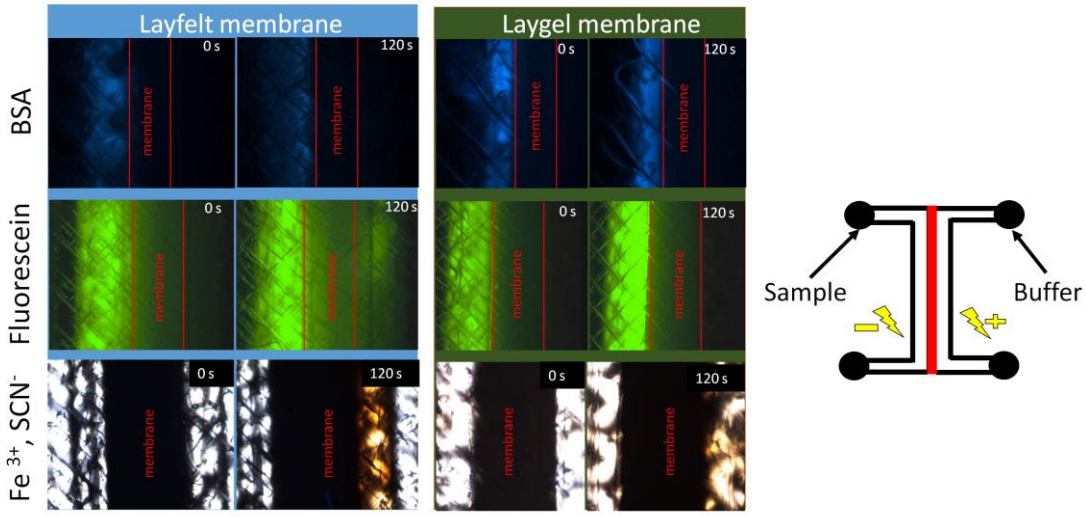

Chapter 7

Conclusions and future directions

Integrated microfluidic devices were developed for point-of-collection analysis of complex biological and environmental samples. These are conventionally performed in a central laboratory by highly trained professionals, requiring bulky and expensive instrumentation, large amounts of reagent and sample consumption, and are time-consuming due to tedious manual procedures. The developed integrated microfluidic devices achieved sample-in/answer-out analysis without sample pre-treatment for direct analysis of HSA in urine, drugs in blood, and nitrate in soil.

In chapter 3, a PDMS microfluidic device with two integrated commercially available PCTE membranes were developed for automated and fast diagnosis of (micro) albuminuria with a LOD of 1.5 μg/mL. Two PDMS slabs with microchannels embedded were constructed *via* soft lithography, and then two membranes with different sizes (100 nm, 10 nm) were integrated by sandwiching the membranes in between two PDMS slabs. A size and mobility trap was formed between these two integrated membranes when the voltage was applied, allowing proteins to be concentrated and purified simultaneously based on the size-selective filtering of the membranes.

Recognising the difficulty in making these devices, the focus shifted to 3D printing for fast prototyping of integrated microfluidic devices. 3D printing shows much potential for microfluidics, particularly for the fabrication of complex, integrated devices. FDM printers with multiple extruders provide a new approach for the

fabrication of multi-material devices with unprecedented simplicity, benefiting from the rapid development of various functional materials. In Chapter 4, a microfluidic device with an integrated membrane and embedded liquid reagents was fabricated by multi-material FDM 3D printing in one step. The microfluidic chip body and membrane were printed using different materials from different extruders. The analytical use of the integrated device was demonstrated by colorimetric determination of nitrate from soil using the Griess reaction, eliminating the need for filtration/centrifugation.

Fluidic flow behaviour in microchannel is of great importance during flow-based analysis, such as microchip electrophoresis. Prior to being used in electrophoresis based analysis, the fluidic behaviour of 3D printed microfluidic device was investigated. In this part, fluid mixing behaviour was examined using microfluidic devices printed with a FDM printer using various FDM printing orientations (0°, 30°, 60°, 90°) of the filament to the direction of the fluid flow. The FDM printed devices with 60° orientation showed the highest mixing efficiency, while 0° and 90° orientations printed chips with least mixing, thus more laminar fluidic behaviour. The results demonstrated that the FDM printing orientation provides a simple means to control fluidic behaviour in microfluidic devices. So devices printed with 0° and 90° orientations will be more suitable for electrophoretic separation when convective mixing is undesirable.

Finally, in Chapter 6, a microfluidic device with integrated membranes and electrode was developed *via* multi-material 3D printing with 0° orientation. Two membranes with different pore sizes were printed with different porous composite filaments, a conductive PLA was used for electrode fabrication. The whole device with integrated functional parts was printed in one step, without any

external assembling. The application of this device was demonstrated by direct analysis of drugs in urine samples without sample treatment, which shows great potential of this device for a portable diagnostic tool for drug monitoring.

Several issues occurred when using a FDM printer to fabricated microfluidic devices fabrication:

1. In chapter 4, to print a seamless membrane without leakage was challenging. For the design, there needed to be some overlap of the membrane (Lay-felt) and chip body (ABS) to get a better sealing joints. When the printing nozzle switched from the ABS nozzle to Lay-felt nozzle, an additional extrusion step was added by modifying the G-code to extrude some Lay-felt material before printing the device to ensure that there was enough Lay-felt material to properly print the membrane. When finishing the Lay-felt membrane printing, the filament was physically retracted in the nozzle by modifying the G-code to add this step which served to alleviate the leakage.

2. In chapter 5, to print chip with accurate channel dimension and better transparency was challenging. Different printing paths resulted in different channel dimension accuracy: when the nozzle moved continuously around the channel to fill the channel wall with appropriate loop numbers, we could get the channel size closer to the designed dimensions. When the loop number was not appropriate, the nozzle moved rapidly to "in-fill" the channel wall, which resulted in the actual channel being smaller than the design. The infill rate, temperature and also the printing speed affected the transparency of the printed structure. Normally a 100% infill rate and slow printing speed was chosen for better transparency.

3. In chapter 6, embedding electrode was challenging. When printing with more than one material, in this case it was four different materials, the nozzle alignment was critical. For electrode embedding, at the beginning, attempts to incorporate the electrode in the chip body resulted in the clear chip body being contaminated by the black conductive material and it was not suitable for the fluorescein detection. This problem was overcome by changing the design with the reservoir printed with conductive material as electrodes. By doing this we were able to avoid the crossing of the conductive material printing with other material printing, then a clear chip body was printed. While this proved to be a practical solution to the problems in this instance, it is not viable for future conceivable designs and is a problem that needs to be overcome.

It should be noted that further research for future direction is essential in the following areas:

1. In the first part, the device was only used for protein detection due to the size limitation of second membrane (10 nm). Smaller size membranes (<10 nm) are needed for smaller molecules, such as drug molecules or other small biomarkers in body fluids using this device.

2. In the second part, Griess reagent in absolute ethanol was embedded in the printed chip, and stored for 4 days. However, the sensitivity of using this reagent was very low and the LOD higher than the level required to detect nitrate in soil, making it not practically useful. Further reagent or solvent development is required for this to become practically useful. Additionally, a digital camera was used for taking images, still compromising its portability. Integrating the device with a smartphone camera detection system would enhance its portability.

3. In the third part, we only investigated the basics of the fluid behavior in 3D printed devices with different orientations. It showed very high mixing efficiency when printing with 60° orientation. The use of this as a micromixer for biochemical assays when rapid mixing was desired is one possible way to utilise this design effectively.

4. In the last chapter, different physical and chemical functionalities could be integrated into one chip *via* multimaterial 3D printing. Future directions in this part include, developing new materials with different functionalities, improving the resolution of the FDM printer for smaller microchannel fabrication, increasing the printing speed for mass production of the integrated device, exploiting other printers (SLA, Inkjet printers) for integrated microfluidic devices fabrication.